

DOKSHITZER–GRIBOV–LIPATOV–ALTARELLI–PARISI  
EVOLUTION EQUATIONS

Petja Paakkinen  
October 29, 2015

MASTER'S THESIS



UNIVERSITY OF JYVÄSKYLÄ  
DEPARTMENT OF PHYSICS

Supervisors: Prof. Kari J. Eskola, Dr. Hannu Paukkunen



## Abstract

When calculating scattering probabilities in high momentum transfer hadronic processes perturbatively in quantum chromodynamics (QCD) we find we have to parametrize our ignorance of the hadron structure into so called parton distribution functions (PDF). Even though we cannot derive these parton distributions through perturbation theory, we are able to find analytically the Dokshitzer–Gribov–Lipatov–Altarelli–Parisi (DGLAP) equations which govern their scale evolution.

By considering deeply inelastic lepton–hadron scattering (DIS) we see that in massless QCD collinear divergences are produced. Including these divergent terms into the definitions of parton distributions leads to finite physical quantities and to the DGLAP evolution. In this thesis we derive the DGLAP equations and the related Altarelli–Parisi splitting functions to the leading logarithmic accuracy.

## Tiivistelmä

Laskettaessa suuren liikemäärävaihdon hadronisten prosessien sirontatodennäköisyyksiä häiriöteoreettisesti kvanttiväridynamiikan (QCD) avulla joudumme parametrisoimaan tietämättömyyttämme hadronien rakenteesta nk. partonijakaumafunktioihin (PDF). Vaikka nämä partonijakaumat eivät ole johdettavissa häiriöteoreettisesti, voidaan niiden skaalaevoluutiota määrittävät Dokshitzer–Gribov–Lipatov–Altarelli–Parisi (DGLAP) -yhtälöt löytää analyyttisellä laskulla.

Tarkastelemalla syvästi epäelastista leptoni–hadroni sirontaa (DIS) näemme massattoman QCD:n tuottavan kollineaarisia divergenssejä. Näiden divergenttien termien sisällyttäminen partonijakaumien määritelmään johtaa fysikaalisesti äärellisiin suureisiin ja DGLAP-yhtälöiden mukaiseen skaalaevoluutioon. Tässä työssä johdetaan DGLAP-yhtälöt ja niihin liittyvät Altarelli–Parisi-jakautumisfunktiot johtavaan logaritmiseen kertalukuun.



# Foreword

This thesis encompasses my current knowledge and understanding of the scale evolution of parton distributions in hadrons. I am grateful for guidance from Prof. Kari J. Eskola and Dr. Hannu Paukkunen who have supervised this work. Paukkunen's PhD thesis [1] has been an excellent introduction to the subject. In there it is shown how one can neatly derive DGLAP evolution equations through resummation of initial state collinear divergences. By the used method one can very effectively find the splitting functions for gluon to gluon and quark to gluon transitions, which are hard to achieve by other means. The discussion here follows quite similar lines, but in more details at places.

During the process of writing this thesis I also tried to extend the derivation to show explicitly the presumed cancellation of other divergences (at least in the first nontrivial order). This appeared to be quite tricky in the chosen calculational machinery (light-cone gauge and Sudakov decomposition with cut-off regulators) and the attempt ended up inconclusive. I would like to thank my supervisors for patience during the time I took to study these matters. Comments from Doc. Tuomas Lappi and Prof. Kimmo Kainulainen have also been helpful.

Let these be my first baby steps on the way towards asymptotic freedom from doubt, or what some people would call the truth.

# Contents

<b>1</b>	<b>Introduction</b>	<b>1</b>
<b>2</b>	<b>Deeply inelastic scattering</b>	<b>3</b>
2.1	Unpolarized cross section . . . . .	4
2.1.1	Structure functions . . . . .	6
2.2	Parton model . . . . .	7
2.2.1	Born approximation . . . . .	8
<b>3</b>	<b>Appearance of collinear divergences</b>	<b>11</b>
3.1	Real gluon emission . . . . .	12
3.1.1	Phase space considerations . . . . .	13
3.1.2	Initial state radiation . . . . .	16
3.1.3	Interference terms . . . . .	17
3.2	Virtual corrections . . . . .	18
3.2.1	Quark self-energy . . . . .	19
3.2.2	Vertex correction . . . . .	25
3.3	Initial gluons . . . . .	27
3.3.1	Scattering from a gluon induced quark . . . . .	27
3.3.2	Interference terms . . . . .	28
3.4	Summation of divergences . . . . .	29
<b>4</b>	<b>Leading logarithm approximation</b>	<b>31</b>
4.1	Two-gluon emission . . . . .	31
4.1.1	Two-rung ladder . . . . .	32
4.1.2	Non-ladder diagrams . . . . .	35
4.2	Additional ladder diagrams . . . . .	36
4.2.1	Vertical line gluons . . . . .	37
4.2.2	Gluon initiated diagrams . . . . .	38
4.2.3	Gluon self-energy . . . . .	40
4.3	Generalization to higher orders . . . . .	44

4.3.1	Redefinition of parton distribution functions . . . . .	46
4.3.2	DGLAP evolution equations . . . . .	46
<b>5</b>	<b>Concluding remarks</b>	<b>49</b>
<b>A</b>	<b>Quantum chromodynamics in the axial gauge</b>	<b>51</b>
A.1	QCD Lagrangian . . . . .	51
A.2	Feynman rules . . . . .	52
A.3	Spin and polarization sums . . . . .	53
A.4	Color algebra . . . . .	54
<b>B</b>	<b>Kinematics</b>	<b>55</b>
B.1	Sudakov decomposition . . . . .	55
B.2	Transverse momentum tensor integrals . . . . .	56



# Chapter 1

## Introduction

Our current best knowledge of fundamental particles and their interactions is encoded into the standard model of particle physics. In addition to the electromagnetic and weak interactions given by a unified field theory with broken  $U(1) \times SU(2)$  symmetry, we believe the strong force of nature to be best described with  $SU(3)$  symmetric gauge theory called quantum chromodynamics (QCD).

At low energies this strong force binds quarks, fundamental building blocks of matter carrying  $SU(3)$  color charge, into colorless hadrons. This phenomenon, due to which no free quarks are observed in nature, is called *confinement*. To study the internal structure of hadrons, we need a suitable probe for doing so. For this, the deeply inelastic lepton–hadron scattering (DIS) appears to be a good choice. We have only one hadron involved in the initial state and at sufficiently low virtuality scales, the interaction can be mediated solely by a photon.

Contrary to the quantum electrodynamics (QED) where the coupling constant grows towards higher energies (smaller distances), in a non-abelian gauge theory with sufficiently low number of active fermions (QCD), calculations show that we should expect *asymptotic freedom* [2]. The more energetic the scattering is, the more free quarks appear to be from internal interactions and we can no more consider the lepton to scatter off a hadron as one entity, but from an ensemble of its building blocks, named *partons*. These kinds of processes, where due to a large momentum transfer distances smaller than the dimensions of the hadron become important, are called *hard processes*.

The asymptotic freedom of QCD ensures that we can use perturbation theory in calculating hard cross sections. However, care must be taken when terminating

the expansion since higher order Feynman diagrams are plagued by various kinds of divergences. Ultraviolet divergences are known to disappear in the renormalization procedure, but cancellation of soft and collinear divergences depends on the inclusiveness of the process at hand.

In the case of deeply inelastic scattering we find that certain collinear divergences coming from initial state radiation persist and thus have to be computed to all orders in perturbation theory. Luckily, by choosing an appropriate “physical” gauge, leading divergences can be made to appear in only a very limited number of diagrams, which are easily summed up. These *leading logarithms* can then be included to the definition of *parton distribution functions* (PDFs) which become scale dependent in this resummation. In this thesis I will show how one can extract these leading logarithms and how their resummation leads to the *Dokshitzer–Gribov–Lipatov–Altarelli–Parisi* (DGLAP) *evolution equations* [3, 4, 5, 6].

I will be working in four space-time dimensions and with on-shell massless initial and final state partons. This has the advantage that the relevant collinear divergences are clearly visible and do not get mixed with other divergences. However, there are also downsides to this approach. Namely, we do not have a gauge invariant way to regulate ultraviolet divergences (this would require dimensional regularization), for which reason we will not discuss the ultraviolet renormalization to any detail here.

I begin the discussion with the basic notions about DIS and parton model in Chapter 2. In Chapter 3 we turn on the QCD interactions to see the appearance of collinear divergences in the first nontrivial order of the strong coupling constant. The all orders calculation is discussed in Chapter 4 where we also derive the DGLAP equations. Some concluding remarks are given in Chapter 5.

# Chapter 2

## Deeply inelastic scattering

Let us consider the deeply inelastic scattering (DIS) process, where a lepton  $\ell$  scatters off a hadron  $h$ , which breaks into a hadronic multi-particle state  $X$  and we measure the energy and scattering angle of the outgoing lepton  $\ell'$ . Symbolically we may write this as

$$\ell(l) + h(P) \rightarrow \ell'(l') + X(P_X), \quad (2.1)$$

where we wrote in parentheses the four-momenta associated with the particles (or group of particles). In the *fully inclusive* case we do not keep track of the momenta of final state hadrons, but require a true multi-particle final state, hence the name *deeply inelastic*, by demanding the invariant mass of the hadronic state to be much greater than the initial hadron mass,  $W^2 \equiv P_X^2 \gg M^2$ .

Since leptons do not carry color, the interaction is mediated via an electroweak boson with momentum  $q = l - l'$  as shown in the Fig. 2.1. We limit our consideration to the neutral current process, where we have the same lepton

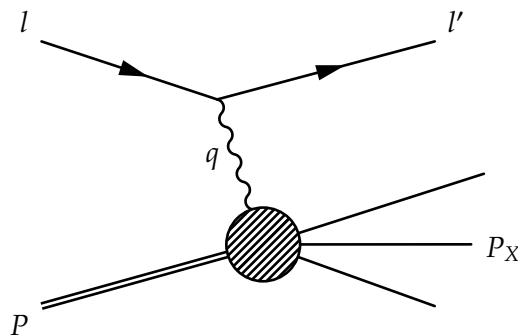


Figure 2.1: Deeply inelastic lepton-hadron scattering.

in the initial and final states ( $\ell = \ell'$ ). At reasonably low momentum transfer, that is, less than the  $Z$ -boson mass,

$$Q^2 \equiv -q^2 = -(l - l')^2 \ll M_Z^2, \quad (2.2)$$

this process is dominated by exchange of one (virtual) photon.

In addition to the momentum transfer  $Q^2$  defined above we will make use of two other Lorentz-invariant variables, the *Bjorken*  $x$

$$x \equiv \frac{Q^2}{2P \cdot q} \quad (2.3)$$

and the inelasticity

$$y \equiv \frac{P \cdot q}{P \cdot l}. \quad (2.4)$$

Together they fully describe the scattering kinematics. In the hadron rest frame, which is often the laboratory frame of the experiment, these variables are expressible as

$$\begin{aligned} Q^2 &= 4EE' \sin^2 \frac{\vartheta}{2}, \\ x &= \frac{Q^2}{2M\nu}, \quad y = \frac{\nu}{E}, \end{aligned} \quad (2.5)$$

where we have neglected the lepton mass and  $E = l^0$  ( $E' = l'^0$ ) is the energy of the incoming (outgoing) lepton,  $\nu = E - E'$  is the amount of energy transferred by the virtual photon and  $\vartheta$  is the lepton scattering angle.

## 2.1 Unpolarized cross section

The unpolarized differential DIS cross section for a lepton plus  $n$ -particle final state is<sup>1</sup>

$$d\sigma_n = \frac{1}{2(S - M^2)} \frac{d^3l'}{(2\pi)^3 2l'^0} \prod_{i=1}^n \frac{d^3\mathbf{k}_i}{(2\pi)^3 2k_i^0} (2\pi)^4 \delta(P + l - l' - \sum_{j=1}^n k_j) \langle |\mathcal{M}^{\ell h \rightarrow \ell X_n}|^2 \rangle, \quad (2.6)$$

where  $S \equiv (l + P)^2$  is the centre of mass energy squared and  $\langle \dots \rangle$  denotes the average over initial and sum over final state spin degrees of freedom.

<sup>1</sup>The discussion in this section follows closely to what was presented in [7].

The matrix element can be read from the QED Feynman rules [8] which give us

$$\mathcal{M}^{\ell h \rightarrow \ell X_n} = i \frac{e^2}{q^2} \bar{u}(l', s') \gamma_\mu u(l, s) \langle X_n(\{k_i\}, \{\sigma_i\}) | \hat{J}^\mu(0) | h(P, \sigma) \rangle, \quad (2.7)$$

where we denote by  $\langle X_n(\{k_i\}, \{\sigma_i\}) | -ie \hat{J}^\mu(0) | h(P, \sigma) \rangle$  the electromagnetic transition current from the initial hadron state with momentum  $P$  and spin  $\sigma$  to the  $n$ -particle final state with momenta  $k_1, \dots, k_n$  and spins  $\sigma_1, \dots, \sigma_n$ . The spinors  $u(l, s)$  and  $\bar{u}(l', s')$  come from having an incoming lepton with spin  $s$  and an outgoing lepton with spin  $s'$ , respectively,  $-ie\gamma_\mu$  is the lepton-photon vertex with  $e$  the electron charge and the  $q^2$  denominator comes from the photon propagator.

Now, for the inclusive cross section, we have to integrate over  $d^3\mathbf{k}_i$  and sum over  $n$ . We find we may write

$$d\sigma = \frac{1}{2(S - M^2)} \frac{e^4}{q^4} \frac{d^3\mathbf{l}'}{(2\pi)^3 2l'^0} L_{\mu\nu}(l, l') 4\pi M W^{\mu\nu}(P, q), \quad (2.8)$$

where the leptonic tensor  $L_{\mu\nu}$  we are able to write in terms of particle four-momenta (we neglect the lepton mass)

$$L_{\mu\nu}(l, l') \equiv \frac{1}{2} \sum_{s, s'} \bar{u}(l', s') \gamma_\mu u(l, s) \bar{u}(l, s) \gamma_\nu u(l', s') = 2(l_\mu l'_\nu + l'_\mu l_\nu - l \cdot l' g_{\mu\nu}), \quad (2.9)$$

but for the hadronic tensor

$$4\pi M W^{\mu\nu}(P, q) \equiv \frac{1}{2} \sum_{\sigma} \sum_n \sum_{\sigma_1 \dots \sigma_n} \int \prod_{i=1}^n \frac{d^3\mathbf{k}_i}{(2\pi)^3 2k_i^0} (2\pi)^4 \delta(P + q - \sum_{j=1}^n k_j) \times \langle h(P, \sigma) | \hat{J}^{\nu}(0) | X_n(\{k_i\}, \{\sigma_i\}) \rangle \langle X_n(\{k_i\}, \{\sigma_i\}) | \hat{J}^{\mu}(0) | h(P, \sigma) \rangle \quad (2.10)$$

this task remains yet unsolved, since we have not discussed a way to compute the transition currents. To this end, we need to model the structure of the hadron in a way or another. We shall do this with the *parton model* as described in Sec. 2.2.

In terms of the Lorentz-invariant variables  $Q^2$ ,  $x$  and  $y$  we have

$$\frac{d^3\mathbf{l}'}{(2\pi)^3 2l'^0} = \frac{1}{16\pi^2} \frac{y}{x} dQ^2 dx, \quad (2.11)$$

whereby we may write the Lorentz-invariant double differential cross section

$$\frac{d\sigma}{dQ^2 dx} = \frac{4\pi\alpha^2}{Q^4} \frac{yM}{2x(S - M^2)} L_{\mu\nu}(l, l') W^{\mu\nu}(P, q), \quad (2.12)$$

where  $\alpha \equiv e^2/4\pi$  is the fine-structure constant.

## 2.1.1 Structure functions

Using the translation properties<sup>2</sup> of the fields and states and completeness of the  $|X_n\rangle$  states, we can simplify Eq. (2.10) into a form

$$W^{\mu\nu}(P, q) = \frac{1}{4\pi M^2} \frac{1}{2} \sum_{\sigma} \int d^4x e^{-iq \cdot x} \langle h(P, \sigma) | \hat{j}^{\nu}(0) \hat{j}^{\mu}(x) | h(P, \sigma) \rangle. \quad (2.13)$$

Contracting this with  $q_{\mu}$  gives us

$$\begin{aligned} q_{\mu} W^{\mu\nu}(P, q) &= i \frac{1}{4\pi M^2} \frac{1}{2} \sum_{\sigma} \int d^4x \partial_{\mu} \left( e^{-iq \cdot x} \langle h(P, \sigma) | \hat{j}^{\nu}(0) \hat{j}^{\mu}(x) | h(P, \sigma) \rangle \right) \\ &\quad - i \frac{1}{4\pi M^2} \frac{1}{2} \sum_{\sigma} \int d^4x e^{-iq \cdot x} \langle h(P, \sigma) | \hat{j}^{\nu}(0) \partial_{\mu} \hat{j}^{\mu}(x) | h(P, \sigma) \rangle, \end{aligned} \quad (2.14)$$

where the first term is a four-surface integral, which vanishes since we expect the electromagnetic current to go to zero infinitely far from the interaction point, and the second term contains a four-divergence  $\partial_{\mu} \hat{j}^{\mu}(x)$ , which is zero by the conservation of the electromagnetic current. Hence we have

$$q_{\mu} W^{\mu\nu}(P, q) = 0. \quad (2.15)$$

Now, since the leptonic tensor Eq. (2.9) is symmetric in exchange of the Lorentz indices, only the symmetric part of  $W^{\mu\nu}$  will survive the contraction  $L_{\mu\nu} W^{\mu\nu}$ . We can thus neglect any antisymmetric parts of the hadronic tensor and write in the most general symmetric form satisfying Eq. (2.15)

$$W^{\mu\nu}(P, q) = -W_1(P, q) \left( g^{\mu\nu} - \frac{q^{\mu} q^{\nu}}{q^2} \right) + \frac{W_2(P, q)}{M^2} \left( P^{\mu} - \frac{P \cdot q}{q^2} q^{\mu} \right) \left( P^{\nu} - \frac{P \cdot q}{q^2} q^{\nu} \right), \quad (2.16)$$

where  $W_1$  and  $W_2$  are Lorentz-invariant *structure functions*. We can contract this with the leptonic tensor

$$L_{\mu\nu} W^{\mu\nu} = W_1(4l' \cdot l) + \frac{W_2}{M^2}(4P \cdot l P \cdot l' + P^2 q^2) \quad (2.17)$$

to obtain the following expression for the cross section

$$\frac{d\sigma}{dQ^2 dx} = \frac{4\pi\alpha^2}{Q^4} \frac{1}{x} \left\{ F_1(x, Q^2) xy^2 + F_2(x, Q^2) \left( 1 - y - xy \frac{M^2}{S - M^2} \right) \right\}, \quad (2.18)$$

---

<sup>2</sup>See e.g. [9] p. 34–35.

where we defined the dimensionless structure functions

$$F_1(x, Q^2) \equiv MW_1, \quad F_2(x, Q^2) \equiv vW_2. \quad (2.19)$$

In the limit where  $M^2 \ll Q^2$  we can obtain these from the hadronic tensor with

$$\begin{aligned} F_2 &= x \left( -g_{\mu\nu} + \frac{12x^2}{Q^2} P_\mu P_\nu \right) MW^{\mu\nu}, \\ F_1 &= \frac{F_2}{2x} - \left( \frac{4x^2}{Q^2} P_\mu P_\nu \right) MW^{\mu\nu}. \end{aligned} \quad (2.20)$$

## 2.2 Parton model

In the parton model, introduced in [10, 11], one pictures the hadron to be an ensemble of pointlike constituents, *partons* (quarks and gluons), from which the lepton scatters incoherently. For such a picture to hold, the scattering has to be instantaneous in the sense that the interaction times between partons become much longer than the time in which the hard scattering occurs. This is certainly true in a frame where the hadron is moving very fast, the *infinite momentum frame*, of which the lepton-hadron center of mass frame is a good approximation at high energies. In the said frame the hadron is Lorentz-contracted and the lifetimes of virtual states are strongly dilated so that the partonic structure of the hadron is frozen for the short period of time it takes for the lepton to pass through it.

We can thus view the DIS cross section as a sum of elastic partonic scatterings

$$d\sigma(P, q) = \sum_i \int d\xi f_i(\xi) d\hat{\sigma}_i(p, q), \quad p = \xi P, \quad (2.21)$$

where  $f_i$  is a *parton distribution function* with the interpretation that  $d\xi f_i(\xi)$  is the mean number of partons “ $i$ ” in the momentum interval  $[\xi P, (\xi + d\xi)P]$ . The differential partonic cross section is

$$d\hat{\sigma}_i = \frac{1}{2\hat{s}} \frac{d^3\mathbf{l}'}{(2\pi)^3 2l'^0} \int \frac{d^3\mathbf{p}'}{(2\pi)^3 2p'^0} (2\pi)^4 \delta(p + l - l' - p') \left\langle |\mathcal{M}^{li \rightarrow li}|^2 \right\rangle, \quad (2.22)$$

where we have assigned momentum  $p'$  with the outgoing parton and the center of mass energy squared of the lepton-parton system is  $\hat{s} \equiv (l + p)^2 = \xi S$

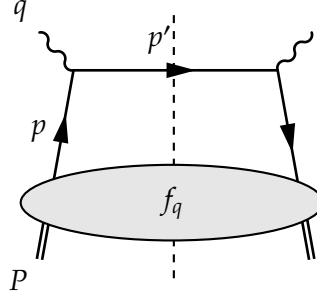


Figure 2.2: Hadronic part of the scattering in parton model.

when neglecting all the masses. In a similar fashion as with the hadronic cross section we can single out the leptonic part and write

$$d\hat{\sigma}_i = \frac{1}{2\hat{s}} \frac{e^4}{q^4} \frac{d^3\mathbf{l}'}{(2\pi)^3 2l'^0} L_{\mu\nu}(l, l') 4\pi M \hat{W}_i^{\mu\nu}(p, q). \quad (2.23)$$

where we have now defined the partonic tensor  $\hat{W}_i$ .

Comparing the above equations with Eq. (2.8) and assuming that  $M^2$  is small compared to  $S$ , we find we can associate

$$W^{\mu\nu}(P, q) = \sum_i \int \frac{d\xi}{\xi} f_i(\xi) \hat{W}_i^{\mu\nu}(p, q). \quad (2.24)$$

This can be viewed pictorially as in Fig. 2.2, where we have adopted the cut diagram notation [12]. Here objects on the left hand side of the cut contribute to the scattering amplitude and on the right hand side to its complex conjugate, whereas the objects extending over the cut (like  $f_q$  here) are probability-like. Cut lines in the middle are understood to be on-shell final state particles.

## 2.2.1 Born approximation

In Fig. 2.2 the parton lines are of course quarks since photon does not couple to gluons. We have neglected all strong interactions as suggested by the asymptotic freedom. In this leading order (LO), or “Born”, approximation the partonic tensor is

$$4\pi M \hat{W}_{q, \text{Born}}^{\mu\nu} = \int d[\text{PS}]_1 \frac{1}{e^2} \left\langle |\mathcal{M}^{\gamma^* q \rightarrow q}|^2 \right\rangle_{\text{Born}}^{\mu\nu}, \quad (2.25)$$

where, since we are now dealing with colored particles, we have promoted  $\langle \dots \rangle$  to include also the average over initial and sum over final state color

(in addition to spin) and we have introduced the notation for *relativistically invariant n-body phase space element*

$$d[\text{PS}]_n \equiv \prod_{i=1}^n \frac{d^3\mathbf{k}_i}{(2\pi)^3 2k_i^0} (2\pi)^4 \delta(p + q - \sum_{j=1}^n k_j). \quad (2.26)$$

Now, in the simplest case of one-particle final state we just have

$$d[\text{PS}]_1 = 2\pi d^4p' \theta(p'^0) \delta(p'^2) \delta(p + q - p') = 2\pi \frac{x}{Q^2} \delta(\xi - x), \quad (2.27)$$

that is, in the LO, the Bjorken  $x$  measures the longitudinal fraction of hadron momentum carried by the parton.

The square of the matrix element is obtained from the Feynman rules, yielding for massless quarks

$$\frac{1}{e^2} \left\langle |\mathcal{M}^{v^*q \rightarrow q}|^2 \right\rangle_{\text{Born}}^{\mu\nu} = \frac{e_q^2}{2} \text{Tr}[\not{p}\gamma^\nu \not{p}'\gamma^\mu], \quad (2.28)$$

where  $e_q$  is the fractional quark charge and  $p' = p + q = q + \xi P$ . Thus the hadronic tensor in the (quark) parton model is

$$W_{\text{Born}}^{\mu\nu} = \sum_q \int_0^1 \frac{d\xi}{\xi} f_q(\xi) \hat{W}_{q,\text{Born}}^{\mu\nu} = \frac{x}{4MQ^2} \text{Tr}[\not{P}\gamma^\nu (q + x\not{P})\gamma^\mu] \sum_q e_q^2 f_q(x). \quad (2.29)$$

We have here supposed that the initial parton is a quark, but it could be as well an antiquark. This would correspond to reversing the fermion line direction in Fig. 2.2, or exchanging  $\mu$  and  $\nu$  in above formulae. But since the hadronic tensor is symmetric, we can effectively take antiquarks into account by saying that the summation over  $q$  in Eq. (2.29) (and from here on) should go over antiquarks as well.

Neglecting the target mass we now obtain from Eq. (2.20) the structure functions in the parton model,

$$2xF_1(x) = F_2(x) = x \sum_q e_q^2 f_q(x). \quad (2.30)$$

Thus we find that in the parton model the structure functions are only functions of  $x$  and do not depend on  $Q^2$  at all, a phenomenon called *Bjorken scaling*. Further, from Eq. (2.18), we thus have the parton model prediction for the DIS cross section

$$\left( \frac{d\sigma}{dQ^2 dx} \right)_{\text{LO}} = \sum_q e_q^2 f_q(x) \left( \frac{d\hat{\sigma}}{dQ^2 dx} \right)_{\text{Born}}, \quad (2.31)$$

with the partonic Born level cross section

$$\left(\frac{d\hat{\sigma}}{dQ^2 dx}\right)_{\text{Born}} = \frac{4\pi\alpha^2}{Q^4} \left\{ \frac{y^2}{2} + \left(1 - y - xy \frac{M^2}{S - M^2}\right) \right\}. \quad (2.32)$$

# Chapter 3

## Appearance of collinear divergences

The result obtained in Sec. 2.2.1 would have been the end of the discussion if quarks did not interact with each other. But we should expect that the same strong interaction which binds quarks into hadrons will affect the scattering dynamics. Asymptotic freedom, through the smallness of the coupling constant, ensures that these QCD interactions can be treated as small corrections in perturbation theory, and the “naive” parton model result of the previous section could be seen as a good first approximation. However, there are certain corrections that we can not swipe under the carpet since they become infinitely large for massless QCD. We discuss the appearance of such (collinear) divergences in this chapter.

### Gauge choice

Derivation of the gluon propagator requires fixing the gauge in which computations are to be done. As we will see, a probabilistic interpretation of the divergent contributions will require use of a special “physical” gauge. Our choice is the axial gauge as formulated in App. A, with the gauge-fixing vector set to be

$$n \equiv q + xP = q + \frac{x}{\xi} p. \quad (3.1)$$

Notice that this vector coincides with the out going quark momentum in the Born amplitude, Eq. (2.28). It also by definition satisfies  $n^2 = 0$ , which along with a gauge parameter choice  $\lambda = 0$  specifies the *light-cone gauge*. In this

gauge, the gluon propagator introduced in Eq. (A.7) reduces to

$$D_{\alpha\beta}^{ab}(k) = \delta^{ab} \frac{i}{k^2 + i\epsilon} d_{\alpha\beta}(k), \quad d_{\alpha\beta}(k) = -g_{\alpha\beta} + \frac{k_\alpha n_\beta + k_\beta n_\alpha}{k \cdot n}. \quad (3.2)$$

At times, it is convenient to split the propagator into two parts

$$d_{\alpha\beta}(k) = d_{\alpha\beta}^{\text{Feynman}} + d_{\alpha\beta}^{\text{Axial}}(k) \quad (3.3)$$

with

$$d_{\alpha\beta}^{\text{Feynman}} = -g_{\alpha\beta}, \quad d_{\alpha\beta}^{\text{Axial}}(k) = \frac{k_\alpha n_\beta + k_\beta n_\alpha}{k \cdot n} \quad (3.4)$$

denoting the part identical to the Feynman gauge propagator and an additional axial contribution.

This gauge is physical in the sense that only transverse polarizations propagate. It is also free of Faddeev–Popov ghosts [13, 14]. The two physical polarization states  $\varepsilon_\mu(k, \lambda)$  ( $k^2 = 0$ ,  $\lambda = 1, 2$ ) obey a sum rule

$$\sum_{\text{pol.}} \varepsilon_\mu(k) \varepsilon_\nu^*(k) = -g_{\mu\nu} + \frac{k_\mu n_\nu + k_\nu n_\mu}{k \cdot n} = d_{\alpha\beta}(k) \quad (3.5)$$

as shown in App. A.3.

### 3.1 Real gluon emission

Let us consider the process where the quark emits a gluon before or after the scattering. The relevant cut diagrams are shown in Fig. 3.1. We notice that these diagrams contain intermediate propagators which diverge at the on-shell limit<sup>1</sup>

$$\begin{aligned} t^2 &= (p - k)^2 = -2p^0 k^0 (1 - \cos \theta) \rightarrow 0, \\ s^2 &= (p' + k)^2 = 2p'^0 k^0 (1 - \cos \theta') \rightarrow 0. \end{aligned} \quad (3.6)$$

This happens if either of the final state particle energy vanishes,  $k^0, p'^0 \rightarrow 0$ , which we call a *soft* divergence, or if the gluon is emitted along the direction of the incoming or outgoing quark,  $\theta, \theta' \rightarrow 0$ , and we talk about a *collinear* divergence<sup>2</sup>.

<sup>1</sup>Notice here that  $t$  and  $s$  are momentum vectors and are not to be confused with the Mandelstam variables [15].

<sup>2</sup>Often the name *mass divergence* is used for collinear divergences since they appear at the limit of vanishing quark mass.

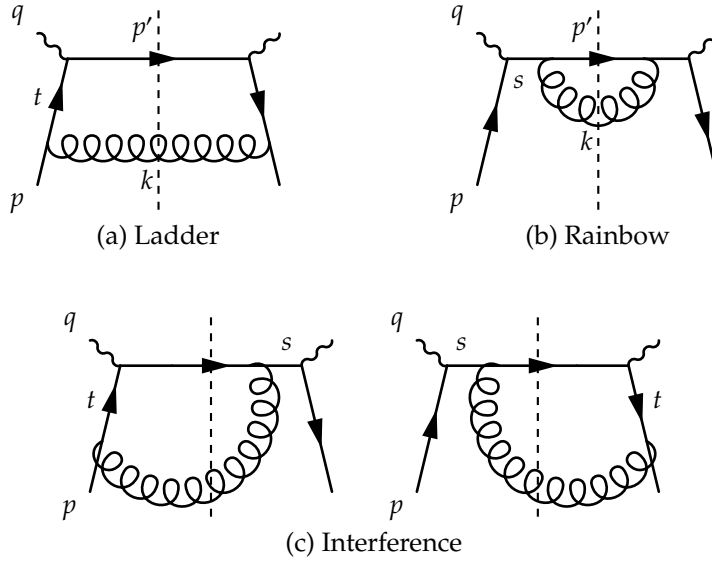


Figure 3.1: Real gluon emission corrections to the quark scattering.

### 3.1.1 Phase space considerations

To extract the transverse degrees of freedom, we apply the Sudakov decomposition [16] as described in App. B.1 to the gluon momentum

$$k = (1 - z)p + \beta n + k_{\perp}. \quad (3.7)$$

Now, since we have  $k^2 = 0$ , these variables are related by

$$\mathbf{k}_{\perp}^2 = -k_{\perp}^2 = 2(1 - z)\beta p \cdot n \quad (3.8)$$

and from  $p'^2 = 0$  we also have

$$(1 - z) = \left(1 - \frac{x}{\xi}\right)(1 - \beta). \quad (3.9)$$

The transverse components of the gluon momentum thus vanish ( $\mathbf{k}_{\perp}^2 \rightarrow 0$ ) at three distinct limits:

1.  $\beta \rightarrow 0$ ,  $\xi \rightarrow \frac{x}{z}$ , for any  $z$ , corresponding to the limit where the gluon is emitted collinearly to the direction of the incoming quark (soft when  $\xi \rightarrow x$ ),
2.  $z \rightarrow 1$ ,  $\xi \rightarrow x$ , for any  $\beta$ , corresponding to the limit where the gluon is emitted collinearly to the direction of the outgoing quark (gluon soft when  $\beta \rightarrow 0$ , quark soft when  $\beta \rightarrow 1$ ),

3.  $z \rightarrow 1, \beta \rightarrow 1$ , for any  $\xi$ , corresponding to the limit where the gluon is emitted collinearly to the direction of the gauge vector (coinciding with the outgoing quark when  $\xi \rightarrow x$ ).

In terms of Sudakov variables we write

$$\frac{1}{t^2} = -\frac{1-z}{\mathbf{k}_\perp^2}, \quad \frac{1}{s^2} = \frac{\beta(1-\beta)}{\mathbf{k}_\perp^2} \quad (3.10)$$

to find that these denominators diverge at the limits 1 and 2, respectively (and are finite otherwise). In the Feynman gauge these would be the only collinear divergences but when working in the light-cone gauge we produce also additional ones. The polarization sum Eq. (3.5) contains a denominator

$$\frac{1}{k \cdot n} = \frac{1}{(1-z)p \cdot n} = \frac{2\beta}{\mathbf{k}_\perp^2}, \quad (3.11)$$

which diverges at the limits 2 and 3. Dokshitzer *et al.* [17] have circumvented this problem by using a *planar gauge* where these “spurious”, unphysical divergences are translated to a kinematically inaccessible area. Here we just take for granted that they cancel in the end without affecting the physical cross-section.

One can argue that since we are considering a process inclusive with respect to final state partons, by the Kinoshita–Lee–Nauenberg (KLN) theorem [18, 19], any divergences coming from soft or final state collinear radiation should cancel, but we expect divergences from emission of a gluon along the direction of the incoming quark to persist since we are not including incoming collinear gluons [20]. Thus only the first limit in the above list is relevant to our calculations. In this “forward” collinear region  $(1-z)$  is kept non-zero (except for the soft limit) and we may write

$$\beta = \frac{\mathbf{k}_\perp^2}{2(1-z)p \cdot n} \rightarrow 0 \quad \text{as} \quad \mathbf{k}_\perp^2 \rightarrow 0. \quad (3.12)$$

By doing so, we are extracting forward collinear divergences into divergent  $\mathbf{k}_\perp^2$ -integrals, whereas other (final state collinear, soft and gauge induced) divergences are contained in divergent  $z$ -integrals.

The differential phase space element for two final state particles can be written in terms of Sudakov variables by the aid of Eq. (B.6) as

$$\begin{aligned} d[\text{PS}]_2 &= \frac{x}{2\xi Q^2} dz \frac{d^2\mathbf{k}_\perp}{(2\pi)^2} \theta(k^0) \theta(p'^0) \\ &\times \delta\left(z^2 - \left(1 + \frac{x}{\xi}\right)z + \frac{x}{\xi} + \frac{x}{\xi} \left(1 - \frac{x}{\xi}\right) \frac{\mathbf{k}_\perp^2}{Q^2}\right), \end{aligned} \quad (3.13)$$

where the delta function appears to have two different solutions

$$z = z_{\pm} = \frac{1}{2} \left\{ \left( 1 + \frac{x}{\xi} \right) \pm \sqrt{\left( 1 - \frac{x}{\xi} \right)^2 - 4 \frac{x}{\xi} \left( 1 - \frac{x}{\xi} \right) \frac{\mathbf{k}_{\perp}^2}{Q^2}} \right\}. \quad (3.14)$$

Since we require  $z$  to be real, the discriminant inside the square root must be positive, and thus

$$\mathbf{k}_{\perp}^2 \leq \frac{\xi - x}{4x} Q^2. \quad (3.15)$$

First of the step functions above gives a kinematical constraint

$$1 - z + \frac{x}{\xi(1-z)} \frac{\mathbf{k}_{\perp}^2}{Q^2} \geq 0, \quad (3.16)$$

which is true only for  $z \leq 1$ .

At the collinear limit the two solutions given in Eq. (3.14) simplify to

$$z_+ = 1 + \mathcal{O}(\mathbf{k}_{\perp}^2), \quad z_- = \frac{x}{\xi} + \mathcal{O}(\mathbf{k}_{\perp}^2), \quad (3.17)$$

and thus we find that  $z_+$  does not contribute to the forward collinear divergence since it would render the  $t^2$  denominator given in Eq. (3.10) nondivergent. We can thus safely set  $z = z_-$  from here on. Actually, the requirement

$$1 - z - \left( \frac{x}{\xi} \right)^2 \frac{\mathbf{k}_{\perp}^2}{Q^2} \geq 0 \quad (3.18)$$

coming from the second step function in Eq. (3.13) holds for  $z = z_1$  strictly speaking only at  $\mathbf{k}_{\perp}^2 = 0$ , or equivalently,  $z_- = x/\xi$ . Hence in the relevant part of the phase space the delta function in Eq. (3.13) may be written as

$$\frac{\delta(z - z_-)}{\left| 2z_- - \left( 1 + \frac{x}{\xi} \right) \right|} = \frac{\xi}{z(1-z)} \delta\left( \xi - \frac{x}{z} \right) \quad (3.19)$$

and we thus have

$$d[\text{PS}]_2 = \frac{x}{Q^2} \frac{dz}{2z(1-z)} \frac{d^2\mathbf{k}_{\perp}}{(2\pi)^2} \delta\left( \xi - \frac{x}{z} \right). \quad (3.20)$$

### 3.1.2 Initial state radiation

After taking the color and spin average, the contribution from the ladder diagram, Fig. 3.1 (a), reads

$$\frac{1}{e^2} \left\langle |\mathcal{M}^{\gamma^* q \rightarrow qg}|^2 \right\rangle_{\text{Ladder}}^{\mu\nu} = g_s^2 \frac{1}{N_C} \text{Tr}[t^a t^a] \frac{e_q^2}{2} \frac{1}{t^4} \sum_{\text{pol.}} \text{Tr}[\not{p} \not{\xi} \not{t} \gamma^\nu \not{p}' \gamma^\mu \not{t} \not{\xi}^*], \quad (3.21)$$

where  $t = p - k$  is the intermediate quark momentum and, by using Eq. (A.15), the color factor can be re-expressed as

$$\frac{1}{N_C} \text{Tr}[t^a t^a] = C_F. \quad (3.22)$$

Using the polarization sum given in Eq. (3.5) we find

$$\sum_{\text{pol.}} \not{\xi}^* \not{p} \not{\xi} = \frac{2}{1-z} (k + \beta \not{h}), \quad (3.23)$$

from which one easily obtains

$$\sum_{\text{pol.}} \not{t} \not{\xi}^* \not{p} \not{\xi} \not{t} = \frac{2}{1-z} \left( \frac{1+z^2}{1-z} \right) \mathbf{k}_\perp^2 \not{p} + \mathcal{O}(\mathbf{k}_\perp^2 k_\perp). \quad (3.24)$$

Putting this back to Eq. (3.21), we observe that in the first term above, the factor  $\mathbf{k}_\perp^2$  cancels with another coming from  $t^4$  leaving single  $\mathbf{k}_\perp^2$  to the denominator, and the higher order terms are not collinearly divergent. The remaining final state quark momentum in the trace can be expressed as

$$p' = n + \mathcal{O}(k_\perp) \quad (3.25)$$

and thus we have

$$\frac{1}{e^2} \left\langle |\mathcal{M}^{\gamma^* q \rightarrow qg}|^2 \right\rangle_{\text{Ladder}}^{\mu\nu} = 4\pi \alpha_s C_F \left( \frac{1+z^2}{1-z} \right) \frac{2(1-z)}{\mathbf{k}_\perp^2} \frac{e_q^2}{2} \text{Tr}[\not{p} \gamma^\nu \not{h} \gamma^\mu] + \dots, \quad (3.26)$$

where the ellipsis contains all the terms nondivergent in the forward collinear limit.

Now, taking the phase space integral we obtain the divergent contribution to the quark tensor

$$\begin{aligned} 4\pi M \hat{W}_{q,\text{Ladder}}^{\mu\nu} &= \int d[\text{PS}]_2 \frac{1}{e^2} \left\langle |\mathcal{M}^{\gamma^* q \rightarrow qg}|^2 \right\rangle_{\text{Ladder}}^{\mu\nu} \\ &= \alpha_s \frac{x}{Q^2} \int_x^1 \frac{dz}{z} C_F \left( \frac{1+z^2}{1-z} \right) \frac{e_q^2}{2} \text{Tr}[\not{p} \gamma^\nu \not{h} \gamma^\mu] \delta\left(\xi - \frac{x}{z}\right) \int_0^{\mathbf{k}_\perp^2 \max} \frac{d\mathbf{k}_\perp^2}{\mathbf{k}_\perp^2} + \dots, \end{aligned} \quad (3.27)$$

where from Eq. (3.15) we have

$$\mathbf{k}_{\perp \max}^2 = \frac{1-z}{4z} Q^2, \quad (3.28)$$

but the lower limit for the transverse momentum is zero making the integral formally infinite. We will regulate the collinear divergence by introducing a cut-off  $\mathbf{k}_{\perp}^2 \geq m^2$ , by which the integral becomes

$$\int_{m^2}^{\mathbf{k}_{\perp \max}^2} \frac{d\mathbf{k}_{\perp}^2}{\mathbf{k}_{\perp}^2} = \log \frac{Q^2}{m^2} + \log \frac{1-z}{4z}. \quad (3.29)$$

Integrating over  $\xi$  we then find the ladder diagram contribution to the hadronic tensor

$$\begin{aligned} W_{Q, \text{Ladder}}^{\mu\nu} &= \sum_q \int_0^1 \frac{d\xi}{\xi} f_q(\xi) \hat{W}_{q, \text{Ladder}}^{\mu\nu} \\ &\stackrel{\text{LL}}{=} \frac{x}{4MQ^2} \text{Tr}[\not{p}\gamma^\nu (q + x\not{p})\gamma^\mu] \sum_q e_q^2 \frac{\alpha_s}{2\pi} \log\left(\frac{Q^2}{m^2}\right) \int_x^1 \frac{dz}{z} C_F \left(\frac{1+z^2}{1-z}\right) f_q\left(\frac{x}{z}\right), \end{aligned} \quad (3.30)$$

where LL on top of the equality sign denotes that we are only including the large “mass” logarithm  $\log(Q^2/m^2)$  and the label Q is added to denote that this contribution comes from summation over initial quarks (and antiquarks) in distinction from the initial gluon contribution which we will calculate in Sec. 3.3. Notice in the  $z$ -integral the lower bound  $z \geq x$  coming from the requirement that  $\xi \leq 1$ , but also that the integral is divergent at the soft  $z \rightarrow 1$  limit. This divergence will get regulated by the inclusion of virtual corrections, which we consider in Sec. 3.2.

### 3.1.3 Interference terms

The rainbow diagram in Fig. 3.1 (b) obviously does not contribute to initial state “forward” collinear divergence, but the interference diagrams in Fig. 3.1 (c), which contain single  $t^2$  denominators might do. These diagrams are but complex conjugates of each other, so it is sufficient to consider only the one on the left hand side, which contributes to the squared matrix element by

$$\frac{1}{e^2} \left\langle |\mathcal{M}^{\gamma^* q \rightarrow qg}|^2 \right\rangle_{\text{Interference}}^{\mu\nu} = g_s^2 C_F \frac{e_q^2}{2} \frac{1}{t^2 s^2} \sum_{\text{pol.}} \text{Tr}[\not{p}\gamma^\nu \not{\epsilon} \not{p}'\gamma^\mu \not{\epsilon}^*], \quad (3.31)$$

where we have

$$\frac{1}{t^2 s^2} = -\frac{x}{\xi Q^2} \frac{1-\beta}{\mathbf{k}_\perp^2} \quad (3.32)$$

and thus a collinear divergence is produced only if the trace contains a term without  $k_\perp$ -dependence. In the region where  $k \approx (1-z)p$  it is quite easy to show that no such term exists. First, one notices that

$$t \not{\epsilon}^* \not{p} = 2zp \cdot \epsilon^* \not{p} + \mathcal{O}(k_\perp) \quad (3.33)$$

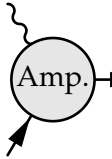
and since the polarization sum contracted with  $p$  yields

$$\sum_{\text{pol.}} p \cdot \epsilon^* \epsilon_\nu = \frac{2\beta}{1-z} n_\nu + \frac{1}{1-z} k_{\perp\nu} = \mathcal{O}(k_\perp), \quad (3.34)$$

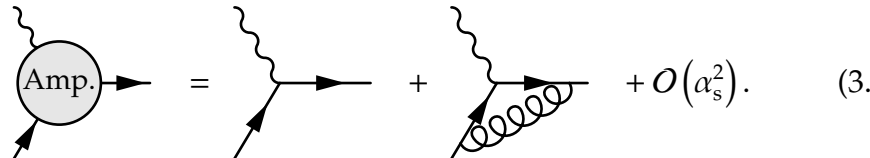
where  $\beta = \mathcal{O}(k_\perp^2)$  as given by Eq. (3.12), the matrix element contains only collinearly nondivergent terms in this kinematical region and thus they do not contribute in the leading logarithmic level here. Notice however the  $1-z$  denominators which can lead to divergences in other kinematical limits.

## 3.2 Virtual corrections

The gluon, real emission of which we considered in the previous section, might as well get reabsorbed by the quark. The short lifetime of this intermediate state allows it to be virtual, with undefined momentum over which we have to integrate. To treat these virtual corrections the right way, we have to use the *LSZ reduction formula* [21], which for the process  $\gamma^* q \rightarrow q$  reads

$$i \mathcal{M}^{\gamma^* q \rightarrow q}(p, q) = \sqrt{Z_q(p)} \sqrt{Z_q(p')} \text{Amp.} \quad (3.35)$$


where “Amp.” refers to sum of all possible amputated diagrams (see below) and  $p' = p + q$ . By an amputated diagram we mean a diagram which cannot be separated into two unconnected parts by removing a single propagator line. Expanding to the order  $\alpha_s$  we have

$$\text{Amp.} = \text{tree} + \text{loop} + \mathcal{O}(\alpha_s^2). \quad (3.36)$$


The *quark field-strength renormalization factor*  $Z_q$  can be found as the multiplicative factor of the one-particle pole of the self-energy corrected propagator

$$Z_q(p) \frac{i\not{p}}{p^2} \underset{p^2 \rightarrow 0}{\sim} \frac{i\not{p}}{p^2} + \frac{i\not{p}}{p^2} [-i\Sigma(p)] \frac{i\not{p}}{p^2} + \dots, \quad (3.37)$$

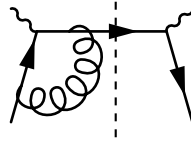
where the symbol  $\sim$  denotes that the poles of both sides are identical<sup>3</sup> and  $\Sigma$  is the *quark self-energy*, which we will compute to the one loop order in Sec. 3.2.1. At leading order we simply have  $Z_q = 1$  and hence we did not need to take it into account in our Born level calculation in Sec. 2.2.1. Moreover, we may write

$$Z_q = 1 + \delta Z_q^{(1)} + \mathcal{O}(\alpha_s^2), \quad (3.38)$$

with  $\delta Z_q^{(1)}$  containing the order  $\alpha_s$  corrections. Squaring Eq. (3.35) we then find that at NLO

$$|\mathcal{M}^{\gamma^* q \rightarrow q}|^2 = \left(1 + \delta Z_q^{(1)}(p) + \delta Z_q^{(1)}(p')\right) |\mathcal{M}^{\gamma^* q \rightarrow q}|_{\text{Born}}^2 + 2 \Re |\mathcal{M}^{\gamma^* q \rightarrow q}|_{\text{VC}}^2 + \mathcal{O}(\alpha_s^2), \quad (3.39)$$

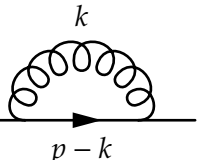
where “VC” refers to vertex correction, diagrammatically

$$|\mathcal{M}^{\gamma^* q \rightarrow q}|_{\text{VC}}^2 = \text{Diagram} \quad (3.40)$$


We shall compute this diagram in Sec. 3.2.2. Since  $\delta Z_q^{(1)}(p')$  contributes only to the cancellation of the singularities in the final state radiation it will be neglected from the present discussion.

### 3.2.1 Quark self-energy

The one-loop quark self-energy diagram reads

$$-i \delta_{ji} \Sigma(p) = i \text{Diagram} \quad (3.41)$$


$$= g_s^2 C_F \delta_{ji} \int \frac{d^4 k}{(2\pi)^4} \frac{\gamma^\alpha (\not{p} - \not{k}) \gamma^\beta}{[(p-k)^2 + i\epsilon][k^2 + i\epsilon]} d_{\alpha\beta}(k),$$

<sup>3</sup>For a more complete treatise on the subject, see *e.g.* [8].

where  $i$  and  $j$  are color indices and in the diagram all momenta are taken to flow from left to right. Using Eq. (3.3) we may write

$$\Sigma(p) = \Sigma^{\text{Feynman}}(p) + \Sigma^{\text{Axial}}(p) \quad (3.42)$$

to denote the part equivalent to the Feynman gauge and an additional axial contribution.

We again exploit the Sudakov decomposition

$$k = \alpha p + \beta n + k_{\perp}, \quad \beta = \frac{k^2 + \mathbf{k}_{\perp}^2 - \alpha^2 p^2}{2\alpha p \cdot n}, \quad (3.43)$$

whereby the denominator coming from quark propagator takes a form

$$(p - k)^2 + i\varepsilon = -\frac{1 - \alpha}{\alpha} \left[ k^2 + \frac{1}{1 - \alpha} \mathbf{k}_{\perp}^2 - \alpha p^2 - i\varepsilon' \right] \quad (3.44)$$

where we used a shorthand notation

$$\varepsilon' \equiv \frac{\alpha}{1 - \alpha} \varepsilon, \quad \begin{cases} \varepsilon' > 0 & \text{if } 0 < \alpha < 1 \\ \varepsilon' < 0 & \text{if } \alpha < 0 \text{ or } \alpha > 1. \end{cases} \quad (3.45)$$

### Feynman part

We can use the decomposition further to obtain

$$d_{\alpha\beta}^{\text{Feynman}} \gamma^{\alpha} (\not{p} - \not{k}) \gamma^{\beta} = -g_{\alpha\beta} \gamma^{\alpha} (\not{p} - \not{k}) \gamma^{\beta} = 2 \left\{ (1 - \alpha) \not{p} - \beta \not{n} - \not{k}_{\perp} \right\}, \quad (3.46)$$

where the term odd in  $k_{\perp}$  vanishes under integration and the Feynman gauge part of the self energy reads

$$\begin{aligned} \Sigma^{\text{Feynman}}(p) &= -i \frac{\alpha_s}{2\pi} C_F \frac{1}{2\pi} \int \frac{d\alpha}{2|\alpha|} dk^2 d\mathbf{k}_{\perp}^2 \frac{\alpha}{1 - \alpha} \frac{1}{[k^2 + \frac{1}{1-\alpha} \mathbf{k}_{\perp}^2 - \alpha p^2 - i\varepsilon'] [k^2 + i\varepsilon]} \\ &\times 2 \left\{ (1 - \alpha) \not{p} - \frac{1}{\alpha} (k^2 + \mathbf{k}_{\perp}^2 - \alpha^2 p^2) \frac{\not{n}}{2p \cdot n} \right\}. \end{aligned} \quad (3.47)$$

Here we note that we can separate the  $k^2$  integral into two parts, one with a  $k^2$  in the numerator and one without. Working out first the latter one, we see that we have two distinct poles in the complex plane. When  $\alpha < 0$  or  $\alpha > 1$  both of these lie in the lower half-plane as shown in the Fig. 3.2 (a). Closing the contour counterclockwise in the upper half-plane no poles get enclosed

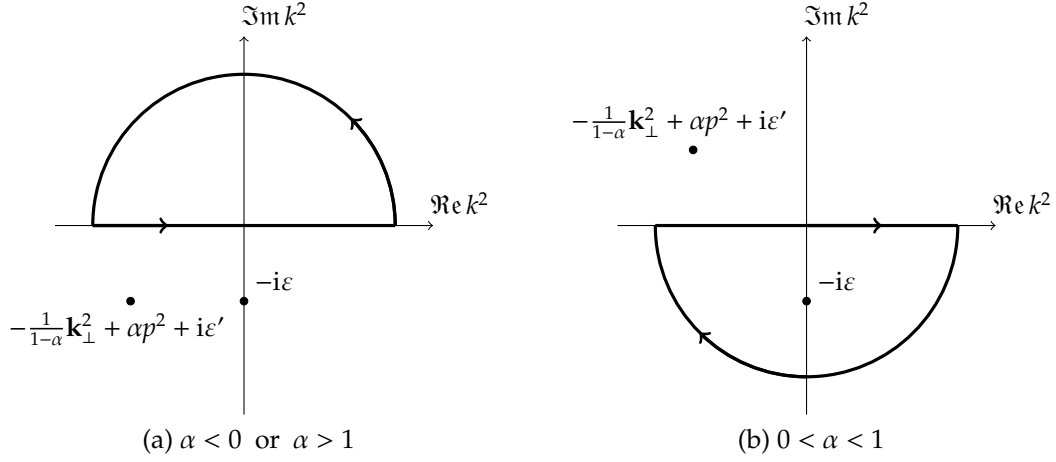


Figure 3.2: The pole structure and integration contours used in Eq. (3.48).

and with the arc integral vanishing when taken to infinity, the integral yields zero for these values of  $\alpha$ .

For  $0 < \alpha < 1$  the pole  $-\frac{1}{1-\alpha}\mathbf{k}_\perp^2 + \alpha p^2 + i\epsilon'$  gets shifted to the upper half-plane. Closing the contour clockwise from the below enclosing the  $-i\epsilon$  pole as shown in Fig. 3.2 (b), we get a nonzero contribution from its residue. Hence we obtain

$$\int_{-\infty}^{\infty} \frac{dk^2}{[k^2 + \frac{1}{1-\alpha}\mathbf{k}_\perp^2 - \alpha p^2 - i\epsilon'][k^2 + i\epsilon]} = \begin{cases} -2\pi i \frac{1-\alpha}{\mathbf{k}_\perp^2 - \alpha(1-\alpha)p^2} & \text{if } 0 < \alpha < 1 \\ 0 & \text{if } \alpha < 0 \text{ or } \alpha > 1. \end{cases} \quad (3.48)$$

Turning our look now on to the integral with an additional  $k^2$  in the numerator, we notice that we cannot perform the contour integral directly, as the arc integral would not vanish. Instead we write

$$\begin{aligned} & \int_{-\infty}^{\infty} dk^2 \frac{k^2}{[k^2 + \frac{1}{1-\alpha}\mathbf{k}_\perp^2 - \alpha p^2 - i\epsilon'][k^2 + i\epsilon]} \\ &= \int_{-\infty}^{\infty} \frac{dk^2}{[k^2 + \frac{1}{1-\alpha}\mathbf{k}_\perp^2 - \alpha p^2 - i\epsilon']} - i\epsilon \int_{-\infty}^{\infty} \frac{dk^2}{[k^2 + \frac{1}{1-\alpha}\mathbf{k}_\perp^2 - \alpha p^2 - i\epsilon'][k^2 + i\epsilon]}, \end{aligned} \quad (3.49)$$

where the result of the second integral on the lower line is just the one given in Eq. (3.48) and the prefactoring  $\epsilon$  takes this term to zero. For the first integral

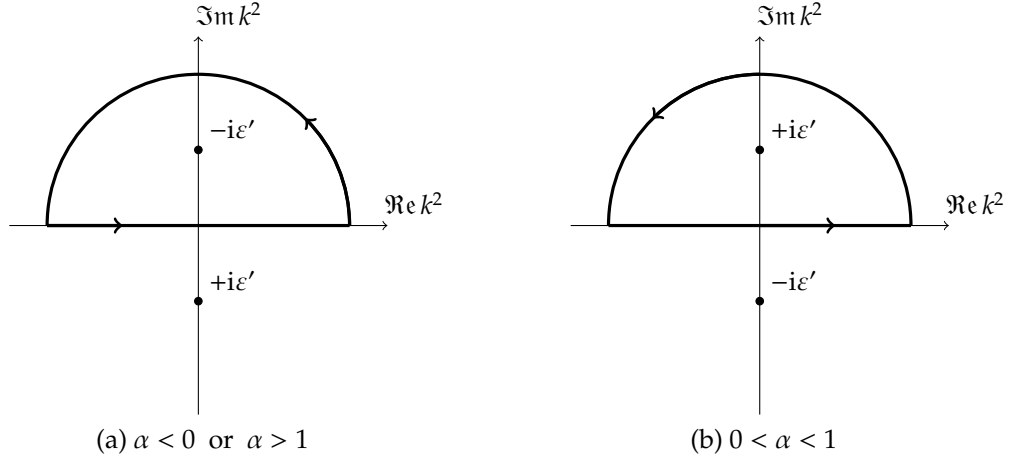


Figure 3.3: The pole structure and integration contours used in Eq. (3.51).

we shift the integration variable  $k^2 \rightarrow k^2 - \frac{1}{1-\alpha} \mathbf{k}_\perp^2 + \alpha p^2$  to obtain

$$\begin{aligned} \int_{-\infty}^{\infty} \frac{dk^2}{[k^2 + \frac{1}{1-\alpha} \mathbf{k}_\perp^2 - \alpha p^2 - i\epsilon']} &= \int_{-\infty}^{\infty} \frac{dk^2}{k^2 - i\epsilon'} = \int_{-\infty}^{\infty} dk^2 \frac{k^2 + i\epsilon'}{(k^2)^2 - (\epsilon')^2} \\ &= i\epsilon' \int_{-\infty}^{\infty} \frac{dk^2}{[k^2 - i\epsilon'][k^2 + i\epsilon']} \end{aligned} \quad (3.50)$$

where in the last equality we dropped the  $k^2$  from the numerator as its contribution vanishes as an odd integral. We have again two poles, locations of which are dependent on the value of  $\alpha$  in a way shown in Fig. 3.3. By closing the contour in the upper half-plane in both cases, a different pole gets enclosed at each time and the sign of the residue changes accordingly. Thus we have

$$\int_{-\infty}^{\infty} dk^2 \frac{k^2}{[k^2 + \frac{1}{1-\alpha} \mathbf{k}_\perp^2 - \alpha p^2 - i\epsilon'][k^2 + i\epsilon]} = \begin{cases} +\pi i & \text{if } 0 < \alpha < 1 \\ -\pi i & \text{if } \alpha < 0 \text{ or } \alpha > 1. \end{cases} \quad (3.51)$$

In Eq. (3.47) this expression is multiplied with  $(|\alpha|(1-\alpha))^{-1}$  and integrated over  $\alpha$ , which gives us

$$\int_{-\infty}^0 \frac{d\alpha (-\pi i)}{|\alpha| 1-\alpha} + \int_0^1 \frac{d\alpha (+\pi i)}{|\alpha| 1-\alpha} + \int_1^{\infty} \frac{d\alpha (-\pi i)}{|\alpha| 1-\alpha}. \quad (3.52)$$

By performing a change of variable  $\alpha \rightarrow 1-\alpha$  one finds that the first integral above just cancels the last one and thus only the integral from 0 to 1 survives.

Combining the results, we have

$$\begin{aligned} \Sigma^{\text{Feynman}}(p) = & -\frac{\alpha_s}{2\pi} C_F \int_0^1 d\alpha \int_0^\infty \frac{d\mathbf{k}_\perp^2}{\mathbf{k}_\perp^2 - \alpha(1-\alpha)p^2} \\ & \times \left\{ (1-\alpha)\not{p} - \frac{1-2\alpha}{2\alpha(1-\alpha)}(\mathbf{k}_\perp^2 + \alpha(1-\alpha)p^2)\frac{\not{n}}{2p \cdot n} \right\}, \end{aligned} \quad (3.53)$$

where the term proportional to  $\not{n}$  is odd in  $\alpha$ -integration and thus vanishes<sup>4</sup>. Performing the  $\mathbf{k}_\perp^2$ -integral for the remaining part we obtain

$$\Sigma^{\text{Feynman}}(p) = -\not{p} \frac{\alpha_s}{2\pi} C_F \int_0^1 d\alpha (1-\alpha) \log\left(\frac{\Lambda^2}{-\alpha(1-\alpha)p^2}\right), \quad (3.54)$$

where we regulated the ultraviolet divergence by a simple cut-off  $\mathbf{k}_\perp^2 < \Lambda^2$ .

### Axial part

We still have to work out the axial contribution. Using the Sudakov decomposition we find

$$d_{\alpha\beta}^{\text{Axial}}(k) \gamma^\alpha (\not{p} - \not{k}) \gamma^\beta = \frac{k_\alpha n_\beta + k_\beta n_\alpha}{k \cdot n} \gamma^\alpha (\not{p} - \not{k}) \gamma^\beta = \frac{4}{\alpha^2} \left( k^2 + \frac{1}{1-\alpha} \mathbf{k}_\perp^2 \right) \frac{\not{n}}{2p \cdot n} + \frac{2}{\alpha} \not{k}_\perp, \quad (3.55)$$

where again the term odd in  $k_\perp$  can be dropped and thus we have

$$\Sigma^{\text{Axial}}(p) = -i \frac{\alpha_s}{2\pi} C_F \frac{1}{2\pi} \int \frac{d\alpha}{2|\alpha|} dk^2 d\mathbf{k}_\perp^2 \frac{4}{\alpha} \frac{k^2 + \frac{1}{1-\alpha} \mathbf{k}_\perp^2}{[k^2 + \frac{1}{1-\alpha} \mathbf{k}_\perp^2 - \alpha p^2 - i\varepsilon'] [k^2 + i\varepsilon]} \frac{\not{n}}{2p \cdot n}. \quad (3.56)$$

The  $k^2$ -integral can be performed as in the Feynman part. This time the  $k^2$ -numerator part given by Eq. (3.51) gets multiplied with  $(|\alpha|\alpha)^{-1}$  and thus contributes with

$$\int_{-\infty}^{-1} \frac{d\alpha}{|\alpha|} \frac{(-\pi i)}{\alpha} + \int_{-1}^0 \frac{d\alpha}{|\alpha|} \frac{(-\pi i)}{\alpha} + \int_0^1 \frac{d\alpha}{|\alpha|} \frac{(+\pi i)}{\alpha} + \int_1^\infty \frac{d\alpha}{|\alpha|} \frac{(-\pi i)}{\alpha}. \quad (3.57)$$

Notice that we have now split the integral into four parts. The first and last ones cancel as before, whereas the two in the middle combine into a symmetric

---

<sup>4</sup>This is expected since in the Feynman gauge  $n$  would be mere an aid for the loop-momentum parametrization and the result should only depend on  $p$ . I thank Dr. Paukkunen for pointing this out.

integral

$$\int_{-1}^0 \frac{d\alpha}{|\alpha|} \frac{(-\pi i)}{\alpha} + \int_0^1 \frac{d\alpha}{|\alpha|} \frac{(+\pi i)}{\alpha} = \pi i \int_{-1}^1 \frac{d\alpha}{\alpha^2} = 2\pi i \int_0^1 \frac{d\alpha}{\alpha^2}. \quad (3.58)$$

Putting this together with the contribution from  $\mathbf{k}_\perp^2$ -numerator part as given by Eq. (3.48) we have

$$\Sigma^{\text{Axial}}(p) = -\frac{p^2}{2p \cdot n} \not{n} \frac{\alpha_s}{2\pi} C_F \int_0^1 d\alpha \frac{2(1-\alpha)}{\alpha} \log\left(\frac{\Lambda^2}{-\alpha(1-\alpha)p^2}\right) \quad (3.59)$$

### Full one-loop propagator

Combining the results, we find that the quark self-energy has the form

$$\Sigma(p) = \Sigma^{\text{Feynman}}(p) + \Sigma^{\text{Axial}}(p) = A\not{p} + B\frac{p^2}{2p \cdot n}\not{n}, \quad (3.60)$$

where  $A$  and  $B$  contain the integrals in Eqs. (3.54) and (3.59) along with  $(\alpha_s/2\pi) C_F$ . Thereby the one-loop corrected propagator becomes

$$\frac{i\not{p}}{p^2} + \frac{i\not{p}}{p^2} [-i\Sigma(p)] \frac{i\not{p}}{p^2} = [1 + A + B] \frac{i\not{p}}{p^2} - B \frac{i\not{n}}{2p \cdot n}. \quad (3.61)$$

The second term is less singular at  $p^2 \rightarrow 0$  (as long as  $p \rightarrow n$ ) and hence the NLO correction to field-strength renormalization factor for the incoming quark with momentum  $p$  is

$$\delta Z_q^{(1)}(p) = A + B = -\frac{\alpha_s}{2\pi} C_F \int_0^1 d\alpha \frac{1+\alpha^2}{1-\alpha} \log\left(\frac{\Lambda^2}{-\alpha(1-\alpha)p^2}\right). \quad (3.62)$$

We can make a further note that at this one-loop order

$$\delta Z_q^{(1)}(p) u(p) = (A + B) u(p) \stackrel{p^2 \rightarrow 0}{=} \frac{i\not{p}}{p^2} [-i\Sigma(p)] u(p), \quad (3.63)$$

so bearing in mind that  $\sqrt{Z_q}(p) = 1 + \frac{1}{2}\delta Z_q^{(1)}(p) + \mathcal{O}(\alpha_s^2)$ , we can diagrammatically express<sup>5</sup> (cf. [22])

$$\sqrt{Z_q}(p) \begin{array}{c} \text{wavy line} \\ \diagup \\ \text{arrow} \end{array} \rightarrow = \begin{array}{c} \text{wavy line} \\ \diagup \\ \text{arrow} \end{array} \rightarrow + \frac{1}{2} \begin{array}{c} \text{wavy line} \\ \diagup \\ \text{arrow} \\ \text{self-energy loop} \end{array} \rightarrow + \mathcal{O}(\alpha_s^2). \quad (3.64)$$

<sup>5</sup>Note here that a naive summation of non-amputated diagrams is not valid since diagrams with self-energy insertions are suppressed by factor of one half.

Identifying the quark virtuality with the cut-off ‘‘mass’’,  $-p^2 = m^2$ , we now extract the large logarithmic self-energy contribution to the hadronic tensor

$$W_{Q,SE}^{\mu\nu} \stackrel{LL}{=} -\frac{x}{4MQ^2} \text{Tr}[\not{p}\gamma^\nu(\not{q} + x\not{p})\gamma^\mu] \sum_q e_q^2 \frac{\alpha_s}{2\pi} \log\left(\frac{Q^2}{m^2}\right) C_F \left(\int_0^1 d\alpha \frac{1+\alpha^2}{1-\alpha}\right) f_q(x), \quad (3.65)$$

where we have neglected the ultraviolet divergent term with  $\log(\Lambda^2/Q^2)$  and all the logarithmic  $\alpha$ -integrals. We will not be concerned about the ultraviolet divergences any further than this, but trust on the *renormalizability* of QCD to ensure that all the physical observables are free from ultraviolet divergences after a proper renormalization of the fields and couplings have been made.

### 3.2.2 Vertex correction

The vertex correction diagram, as given in Eq. (3.40), reads after averaging

$$\frac{1}{e^2} \left\langle |\mathcal{M}^{q \rightarrow q}|^2 \right\rangle_{\text{VC}} = i C_F g_s^2 \frac{e_q^2}{2} \int \frac{d^4k}{(2\pi)^4} \frac{\text{Tr}[\not{p}\gamma^\nu \not{p}'\gamma^\beta (\not{p}' - \not{k})\gamma^\mu (\not{p} - \not{k})\gamma^\alpha]}{[(p' - k)^2 + i\epsilon][(p - k)^2 + i\epsilon][k^2 + i\epsilon]} d_{\alpha\beta}(k), \quad (3.66)$$

where we can immediately take the external quarks to be on-shell, and thus  $p' = n$ . Using the Sudakov decomposition we then find

$$(p - k)^2 + i\epsilon = -\frac{1-\alpha}{\alpha} \left[ k^2 + \frac{1}{1-\alpha} \mathbf{k}_\perp^2 - i\epsilon' \right], \quad \epsilon' = \frac{\alpha}{1-\alpha} \epsilon \quad (3.67)$$

and

$$(p' - k)^2 + i\epsilon = k^2 - 2\alpha p \cdot n + i\epsilon, \quad (3.68)$$

which, we find, gives an additional pole to the  $k^2$ -plane, as shown in Fig. 3.4, compared to the self-energy diagram.

As in Eq. (3.3), we may split  $d_{\alpha\beta}$  into two parts. Using the transverse momentum tensor integrals (B.7) and (B.8) of App. B.2 we obtain

$$-g_{\alpha\beta} \text{Tr}[\not{p}\gamma^\nu \not{p}'\gamma^\beta (\not{p}' - \not{k})\gamma^\mu (\not{p} - \not{k})\gamma^\alpha] = 2 \frac{1-\alpha}{\alpha} \{k^2 + \mathbf{k}_\perp^2 - 2\alpha p \cdot n\} \text{Tr}[\not{p}\gamma^\nu \not{n}\gamma^\mu], \quad (3.69)$$

from where we find the Feynman gauge contribution to be

$$\begin{aligned} \frac{1}{e^2} \left\langle |\mathcal{M}^{q \rightarrow q}|^2 \right\rangle_{\text{VC,Feynman}} &= -i \frac{\alpha_s}{2\pi} C_F \text{Tr}[\not{p}\gamma^\nu \not{n}\gamma^\mu] \frac{1}{2\pi} \int \frac{d\alpha}{2|\alpha|} dk^2 d\mathbf{k}_\perp^2 \\ &\times \frac{2 \{k^2 + \mathbf{k}_\perp^2 - 2\alpha p \cdot n\}}{[k^2 + \frac{1}{1-\alpha} \mathbf{k}_\perp^2 - i\epsilon'][k^2 - 2\alpha p \cdot n + i\epsilon][k^2 + i\epsilon]}. \end{aligned} \quad (3.70)$$

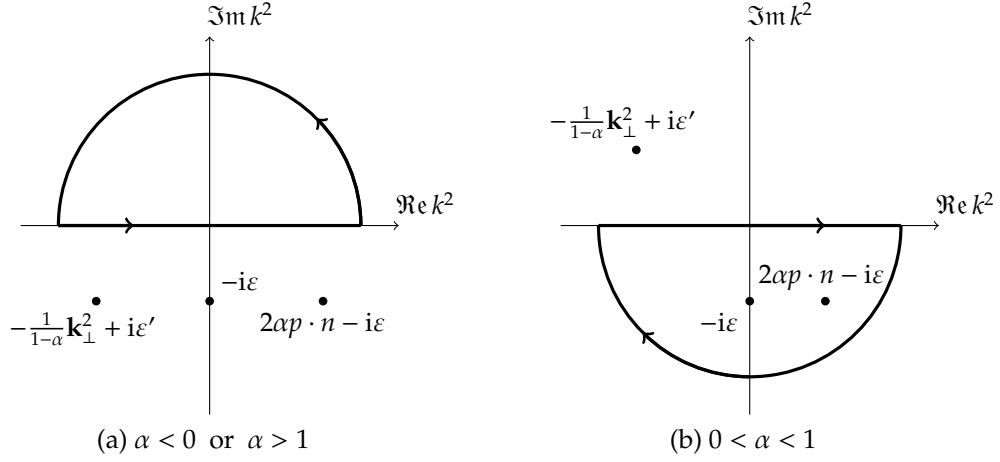


Figure 3.4: The pole structure of the vertex correction diagram.

The three-propagator structure now ensures the vanishing of arc integrals in Fig. 3.4 (a) and (b) even if we have  $k^2$  in the numerator. Again, only the  $0 < \alpha < 1$  part survives and we have

$$\begin{aligned} \frac{1}{e^2} \left\langle |\mathcal{M}^{\gamma^* q \rightarrow q}|^2 \right\rangle_{\text{VC, Feynman}} &= \frac{\alpha_s}{2\pi} C_F \text{Tr}[\not{p}\gamma^\nu \not{q}\gamma^\mu] \int_0^1 d\alpha \frac{1-\alpha}{\alpha} \int_0^{\Lambda^2} d\mathbf{k}_\perp^2 \\ &\times \left\{ \frac{1-\alpha}{\mathbf{k}_\perp^2 + 2\alpha(1-\alpha)p \cdot n} - \frac{1}{\mathbf{k}_\perp^2} \right\}, \end{aligned} \quad (3.71)$$

where the second term in the braces appears to be divergent at the limit  $\mathbf{k}_\perp^2 \rightarrow 0$ . But we have to combine this with the axial part. Dropping once again terms odd in  $k_\perp$  we find

$$\frac{k_\alpha n_\beta + k_\beta n_\alpha}{k \cdot n} \text{Tr}[\not{p}\gamma^\nu \not{p}'\gamma^\beta (\not{p}' - \not{k})\gamma^\mu (\not{p} - \not{k})\gamma^\alpha] = 2 \frac{1-\alpha}{\alpha} \{k^2 - 2\alpha p \cdot n\} \text{Tr}[\not{p}\gamma^\nu \not{q}\gamma^\mu], \quad (3.72)$$

from where we obtain the axial contribution

$$\frac{1}{e^2} \left\langle |\mathcal{M}^{\gamma^* q \rightarrow q}|^2 \right\rangle_{\text{VC, Axial}} = \frac{\alpha_s}{2\pi} C_F \text{Tr}[\not{p}\gamma^\nu \not{q}\gamma^\mu] \int_0^1 d\alpha \frac{1-\alpha}{\alpha} \int_0^{\Lambda^2} \frac{d\mathbf{k}_\perp^2}{\mathbf{k}_\perp^2}, \quad (3.73)$$

which exactly cancels the collinear divergence in Eq. (3.71). Hence the vertex correction does not contribute to the leading logarithm analysis we are after here.

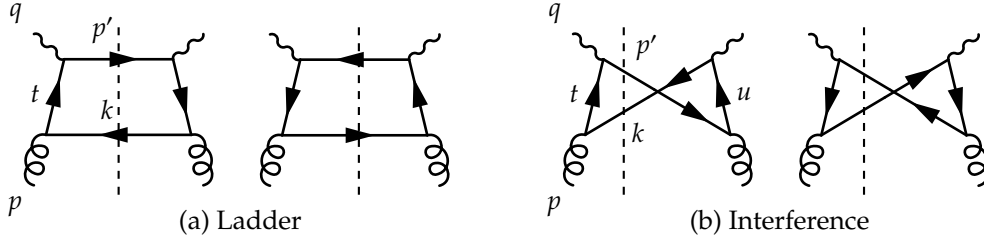


Figure 3.5: Initial gluon contributions to the NLO scattering.

### 3.3 Initial gluons

At the NLO level we have to include also the possibility that the initial parton is a gluon decaying into a quark–antiquark pair from which the lepton scatters. The relevant cut diagrams are shown in Fig. 3.5.

#### 3.3.1 Scattering from a gluon induced quark

Take a look at the left hand side diagram of Fig. 3.5 (a). We denote its contribution to the squared matrix element by

$$\frac{1}{e^2} \left\langle |\mathcal{M}^{\gamma^* g \rightarrow q\bar{q}}|^2 \right\rangle_{\text{Ladder}}^{\mu\nu} = g_s^2 \frac{1}{N_C^2 - 1} \text{Tr}[t^a t^a] \frac{e_q^2}{2} \frac{1}{t^4} \sum_{\text{pol.}} \text{Tr}[k \not{\epsilon} t \gamma^\nu \not{p}' \gamma^\mu t \not{\epsilon}^*], \quad (3.74)$$

where this time, by using Eq. (A.14), the color factor becomes

$$\frac{1}{N_C^2 - 1} \text{Tr}[t^a t^a] = T_F. \quad (3.75)$$

We can use the polarization vector sum to obtain

$$\sum_{\text{pol.}} t \not{\epsilon}^* k \not{\epsilon} t = 2t((1-z)\not{p} + \beta\not{h})t = \frac{2}{1-z} \left( (1-z)^2 + z^2 \right) \mathbf{k}_\perp^2 \not{p} + \mathcal{O}(\mathbf{k}_\perp^2 k_\perp), \quad (3.76)$$

and thus we have

$$\frac{1}{e^2} \left\langle |\mathcal{M}^{\gamma^* g \rightarrow q\bar{q}}|^2 \right\rangle_{\text{Ladder}}^{\mu\nu} = 4\pi \alpha_s T_F \left( (1-z)^2 + z^2 \right) \frac{2(1-z)}{\mathbf{k}_\perp^2} \frac{e_q^2}{2} \text{Tr}[\not{p} \gamma^\nu \not{h}_\perp \gamma^\mu] + \dots \quad (3.77)$$

We may here apply the same phase space element, Eq. (3.20), which we used for the real gluon emission from an initial quark. This gives the following contribution to the partonic tensor

$$\begin{aligned}
4\pi M \hat{W}_{g,\text{Ladder}}^{\mu\nu} &= \int d[\text{PS}]_2 \frac{1}{e^2} \left\langle |\mathcal{M}^{\gamma^* q \rightarrow qg}|^2 \right\rangle_{\text{Ladder}}^{\mu\nu} \\
&= \alpha_s \frac{x}{Q^2} \int_x^1 \frac{dz}{z} T_F \left( (1-z)^2 + z^2 \right) \frac{e_q^2}{2} \text{Tr}[\not{p}\gamma^\nu \not{k}\gamma^\mu] \delta\left(\xi - \frac{x}{z}\right) \int_{m^2}^{Q^2} \frac{d\mathbf{k}_\perp^2}{\mathbf{k}_\perp^2} + \dots
\end{aligned} \tag{3.78}$$

We have already taken into account all the initial gluons in taking the color sum, but the flavor of the final quark is still free and has to be summed over. The contribution to the hadronic tensor thus becomes

$$\begin{aligned}
W_{G,\text{Ladder}}^{\mu\nu} &\stackrel{\text{LL}}{=} \frac{x}{4MQ^2} \text{Tr}[\not{p}\gamma^\nu (\not{q} + x\not{P})\gamma^\mu] \\
&\times \sum_q e_q^2 \frac{\alpha_s}{2\pi} \log\left(\frac{Q^2}{m^2}\right) \int_x^1 \frac{dz}{z} T_F \left( (1-z)^2 + z^2 \right) f_g\left(\frac{x}{z}\right),
\end{aligned} \tag{3.79}$$

where in the summation over  $q$  we are, as before, also including antiquarks and thus the right hand side diagram in Fig. 3.5 (a) has been included here.

### 3.3.2 Interference terms

We still need to consider the interference diagrams in Fig. 3.5 (b) which come with the following kind of contribution to the squared amplitude

$$\frac{1}{e^2} \left\langle |\mathcal{M}^{\gamma^* g \rightarrow q\bar{q}}|^2 \right\rangle_{\text{Interference}}^{\mu\nu} = g_s^2 T_F \frac{e_q^2}{2} \frac{1}{t^2 u^2} \sum_{\text{pol.}} \text{Tr}[k\gamma^\nu \not{p}\not{k}\not{p}'\gamma^\mu \not{t}\not{t}^*], \tag{3.80}$$

where we have only single  $\mathbf{k}_\perp^2$  in the denominator,

$$\frac{1}{t^2 u^2} = -\frac{x(1-x)}{\xi^2 Q^2} \frac{1}{\mathbf{k}_\perp^2}. \tag{3.81}$$

In the trace we have

$$\not{t}\not{k} = 2z(1-z)p \cdot \varepsilon^* \not{p} + \mathcal{O}(k_\perp) \tag{3.82}$$

and the polarization sum gives

$$\sum_{\text{pol.}} p \cdot \varepsilon(p) \varepsilon_\nu(p) = 0. \tag{3.83}$$

Thus no  $\mathbf{k}_\perp^2$ -divergence appears in these diagrams and also for initial gluons the leading logarithm contribution comes from the ladder diagrams.

### 3.4 Summation of divergences

We may now combine the divergent parts found in the previous sections. Summing the initial quark contributions from the ladder diagram and self-energy contributions, Eqs. (3.30) and (3.65), we find

$$W_{\text{Q,NLO}}^{\mu\nu} \stackrel{\text{LL}}{=} \frac{x}{4MQ^2} \text{Tr}[\not{P}\gamma^\nu(\not{q}+x\not{P})\gamma^\mu] \sum_q e_q^2 \frac{\alpha_s}{2\pi} \log\left(\frac{Q^2}{m^2}\right) \int_x^1 \frac{dz}{z} C_F \left(\frac{1+z^2}{1-z}\right)_+ f_q\left(\frac{x}{z}\right), \quad (3.84)$$

where

$$\left(\frac{1+z^2}{1-z}\right)_+ \equiv \left(\frac{1+z^2}{1-z}\right) - \delta(1-z) \int_0^1 d\alpha \frac{1+\alpha^2}{1-\alpha} \quad (3.85)$$

is a so-called *plus distribution* (in general  $g_+$ ), formally defined in integration against a suitably smooth test function  $f$  as

$$\int_0^1 dx g_+(x) f(x) \equiv \int_0^1 dx g(x) (f(x) - f(1)). \quad (3.86)$$

Notice that the  $z$ -integral in Eq. (3.84) is now finite. Let us define a *multiplicative convolution*

$$h \otimes f(x) = \int_x^1 \frac{dz}{z} h(z) f\left(\frac{x}{z}\right) = f \otimes h(x), \quad (3.87)$$

which has a unit element  $1(z) = \delta(1-z)$ ,

$$1 \otimes f(x) = \int_x^1 \frac{dz}{z} \delta(1-z) f\left(\frac{x}{z}\right) = f(x). \quad (3.88)$$

We can then write Eq. (3.84) in a form

$$W_{\text{Q,NLO}}^{\mu\nu} \stackrel{\text{LL}}{=} \frac{x}{4MQ^2} \text{Tr}[\not{P}\gamma^\nu(\not{q}+x\not{P})\gamma^\mu] \sum_q e_q^2 \frac{\alpha_s}{2\pi} \log\left(\frac{Q^2}{m^2}\right) P_{qq} \otimes f_q(x), \quad (3.89)$$

where

$$P_{qq}(z) \equiv C_F \left(\frac{1+z^2}{1-z}\right)_+ \quad (3.90)$$

is the *Altarelli–Parisi splitting function* for quark to quark transition [5]. Since in the light-cone gauge the large logarithmic contributions come only from initial state radiation and not from interference with the outgoing quark, we may interpret

$$\frac{\alpha_s}{2\pi} \log\left(\frac{Q^2}{m^2}\right) P_{qq}(z) \quad (3.91)$$

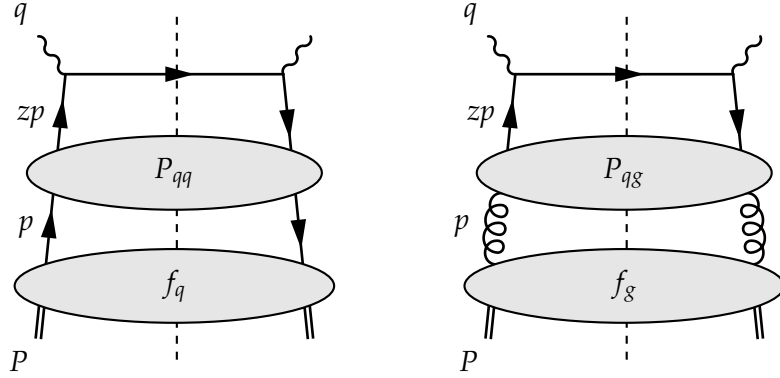


Figure 3.6: The large logarithmic contributions to the hadronic tensor in NLO.

as the probability density for the quark to lose a fraction  $1 - z$  of its momentum by radiating a gluon before interacting with the photon. This probabilistic interpretation would not have been possible in a covariant gauge, where also the interference diagrams give large logarithmic contributions. Similarly for the initial gluon contribution coming from Eq. (3.79) we may write

$$W_{\text{G,NLO}}^{\mu\nu} \stackrel{\text{LL}}{=} \frac{x}{4MQ^2} \text{Tr}[P\gamma^\nu(q + xP)\gamma^\mu] \sum_q e_q^2 \frac{\alpha_s}{2\pi} \log\left(\frac{Q^2}{m^2}\right) P_{qg} \otimes f_g(x), \quad (3.92)$$

with the splitting function for gluon to quark transition

$$P_{qg}(z) \equiv T_F \left( (1-z)^2 + z^2 \right). \quad (3.93)$$

These two large logarithmic contributions to the hadronic tensor can be pictured as in Fig. 3.6, where the splitting functions are understood to be convoluted with the parton distribution below it and to come with the factor  $(\alpha_s/2\pi) \log(Q^2/m^2)$ .

We may now, *a posteriori*, verify our assumption that only divergences coming from emissions along the initial parton line persist after summation of all the relevant diagrams. The splitting functions  $P_{qq}, P_{qg}$  above are exactly the same as those found as coefficients of  $1/\epsilon$  poles in dimensional regularization *after cancellation of all the other divergences* [7, 23]. Combining the above terms with the leading order result from the previous chapter, we find the following  $\mathcal{O}(\alpha_s)$  large logarithm corrected cross section

$$\left( \frac{d\sigma}{dQ^2 dx} \right)_{\text{NLO}} \stackrel{\text{LL}}{=} \sum_q e_q^2 \left\{ \left[ 1 + \frac{\alpha_s}{2\pi} \log\left(\frac{Q^2}{m^2}\right) P_{qq} \right] \otimes f_q(x) + \frac{\alpha_s}{2\pi} \log\left(\frac{Q^2}{m^2}\right) P_{qg} \otimes f_g(x) \right\} \times \left( \frac{d\hat{\sigma}}{dQ^2 dx} \right)_{\text{Born}}. \quad (3.94)$$

# Chapter 4

## Leading logarithm approximation

It should not be a surprise that soft and collinear divergences appear also in higher orders of  $\alpha_s$ . We take a leap of faith and trust our previous assumptions that, order by order, only divergences related to radiation along the direction of the initial parton remain after summing all the diagrams. As we will see, at each order the leading divergence is of the form  $\alpha_s^n \log^n(Q^2/m^2)$  and in the light-cone gauge these *leading logarithms* appear only in ladder type diagrams.

### 4.1 Two-gluon emission

Let us now work our way through a case where an incoming quark emits two gluons before the scattering. We parametrize the gluon momenta as

$$\begin{aligned} k_1 &= (1 - z_1)p + \beta_1 n + k_{1\perp}, & \beta_1 &= \frac{\mathbf{k}_{1\perp}^2}{2(1 - z_1)p \cdot n'}, \\ k_2 &= (1 - z_2)z_1 p + \beta_2 n + k_{2\perp}, & \beta_2 &= \frac{\mathbf{k}_{2\perp}^2}{2(1 - z_2)z_1 p \cdot n'} \end{aligned} \quad (4.1)$$

so that in the context of the ladder diagram Fig. 4.1,  $z_1$  and  $z_2$  are given the interpretation of being fractions of momentum left to the quark at the first and second emission of a collinear gluon, respectively. Using similar arguments as for the two particle final state, the three particle phase space element reduces

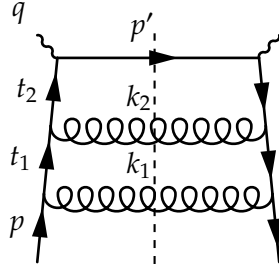


Figure 4.1: Ladder diagram for two-gluon emission.

at the forward (gluons moving to the direction of the initial quark) collinear limit to

$$d[\text{PS}]_3 = \frac{1}{2\pi} \frac{x}{Q^2} \frac{dz_1}{2z_1(1-z_1)} \frac{d^2\mathbf{k}_{1\perp}}{(2\pi)^2} \frac{dz_2}{2z_2(1-z_2)} \frac{d^2\mathbf{k}_{2\perp}}{(2\pi)^2} \delta\left(\xi - \frac{x}{z_1 z_2}\right), \quad (4.2)$$

with  $z_1, z_2 \leq 1$  and  $z_1 z_2 \geq x$ .

Here one should notice that we could as well have the final state gluon with momentum  $k_2$  to come from the lower quark–gluon vertex and the gluon with momentum  $k_1$  to come from the upper vertex, corresponding to a diagram similar to Fig. 4.1 but with the gluon lines crossed both on the left and right hand side of the diagram. Since we are integrating over the momenta and summing over the polarizations and color of the final state gluons, we can switch all the labels and thereby the contribution from this diagram is identical to the ladder diagram in Fig. 4.1.

To avoid counting over the same final state many times we always divide by factorial  $n!$  after integrating over the momenta and summing all the contributions with  $n$  identical particles in the final state [8]. Hence the calculation for emission of two gluons from the initial quark resolves to computing just the contribution from the ladder diagram and the possible interference terms which we treat in Sec. 4.1.2.

### 4.1.1 Two-rung ladder

Let us evaluate the ladder diagram for two-gluon emission given in Fig. 4.1

$$\frac{1}{e^2} \left\langle |\mathcal{M}^{\nu^* q \rightarrow q g g}|^2 \right\rangle_{\text{Ladder}}^{\mu\nu} = g_s^4 \frac{e_q^2}{2} \frac{1}{N_C} \text{Tr}[t^a t^b t^b t^a] \frac{1}{t_1^4 t_2^4} \sum_{\text{pol.}} \text{Tr}[\not{p} \not{\epsilon}_1 t_1 \not{\epsilon}_2 t_2 \gamma^\nu \not{p}' \gamma^\mu t_2 \not{\epsilon}_2^* t_1 \not{\epsilon}_1^*], \quad (4.3)$$

where again from Eq. (A.15) we obtain

$$\frac{1}{N_C} \text{Tr}[t^a t^b t^b t^a] = C_F^2. \quad (4.4)$$

Using the decomposition given in Eq. (4.1) we find

$$\sum_{\text{pol.}} t_1 \not{\epsilon}_1^* \not{p} \not{\epsilon}_1 t_1 = \frac{2}{1-z_1} \left( \frac{1+z_1^2}{1-z_1} \right) \mathbf{k}_{1\perp}^2 \not{p} + \mathcal{O}(\mathbf{k}_{1\perp}^2 k_{1\perp}) \quad (4.5)$$

and further that

$$\sum_{\text{pol.}} t_2 \not{\epsilon}_2^* \not{p} \not{\epsilon}_2 t_2 = \frac{2}{1-z_2} \left( \frac{1+z_2^2}{1-z_2} \right) \mathbf{k}_{2\perp}^2 \not{p} + \mathcal{O}(\mathbf{k}_{2\perp}^2 k_{2\perp}) + \mathcal{O}(k_{1\perp}). \quad (4.6)$$

The final state quark momentum also approaches at the forward collinear limit that of the Born level

$$\not{p}' = \not{p} + \mathcal{O}(k_{1\perp}) + \mathcal{O}(k_{2\perp}). \quad (4.7)$$

Now, as for the one gluon emission, we may write

$$\frac{1}{t_1^2} = -\frac{1-z_1}{\mathbf{k}_{1\perp}^2}, \quad (4.8)$$

but the denominator from upper quark propagator takes a more peculiar form

$$\frac{1}{t_2^2} = -\frac{1-z_2}{\mathbf{k}_{2\perp}^2 + (1-z_1+z_1z_2)\mathbf{k}_{1\perp}^2 + 2(1-z_2)\mathbf{k}_{1\perp} \cdot \mathbf{k}_{2\perp}} \quad (4.9)$$

To perform transverse momentum integrals we will power expand the above expression. In the phase space region where  $\mathbf{k}_{1\perp}^2 < \mathbf{k}_{2\perp}^2$  we have

$$\frac{1}{t_2^2} = -\frac{1-z_2}{\mathbf{k}_{2\perp}^2} \sum_{n=0}^{\infty} \left( (1-z_1+z_1z_2) \frac{1-z_2}{1-z_1} \frac{\mathbf{k}_{1\perp}^2}{\mathbf{k}_{2\perp}^2} + 2(1-z_2) \frac{\mathbf{k}_{1\perp} \cdot \mathbf{k}_{2\perp}}{\mathbf{k}_{2\perp}^2} \right)^n. \quad (4.10)$$

Hence we find the matrix element Eq. (4.3) to be of the form

$$\frac{1}{e^2} \left\langle |\mathcal{M}^{\gamma^* q \rightarrow q g g}|^2 \right\rangle_{\text{Ladder}}^{\mu\nu} = \frac{1}{\mathbf{k}_{1\perp}^2} \frac{1}{\mathbf{k}_{2\perp}^2} \left[ A + B \left( \frac{\mathbf{k}_{1\perp}^2}{\mathbf{k}_{2\perp}^2} \right) + C \left( \frac{\mathbf{k}_{1\perp}^2}{\mathbf{k}_{2\perp}^2} \right)^2 + \dots \right], \quad (4.11)$$

where the ellipsis contains also terms with higher power of  $\mathbf{k}_{1\perp}^2$  in numerator than the  $\mathbf{k}_{2\perp}^2$  in denominator and we are able to neglect any odd powers of  $\mathbf{k}_{1\perp}$

and  $\mathbf{k}_{2\perp}$  since they would integrate to zero. The phase space integration then contains various terms of the following form

$$\int_{m^2}^{Q^2} d\mathbf{k}_{2\perp}^2 \int_{m^2}^{\mathbf{k}_{2\perp}^2} d\mathbf{k}_{1\perp}^2 (\mathbf{k}_{2\perp}^2)^{r-1} (\mathbf{k}_{1\perp}^2)^{s-1} = \begin{cases} \mathcal{O}\left(\log^2\left(\frac{Q^2}{m^2}\right)\right), & \text{if } r = s = 0 \\ \mathcal{O}\left(\log\left(\frac{Q^2}{m^2}\right)\right) + \mathcal{O}\left((m^2)^r\right), & \text{if } r \neq s = 0 \\ \mathcal{O}\left((m^2)^s \log\left(\frac{Q^2}{m^2}\right)\right), & \text{if } r = 0 \neq s \\ \mathcal{O}\left(\log\left(\frac{Q^2}{m^2}\right)\right) + \mathcal{O}\left((m^2)^s\right), & \text{if } r = -s \neq 0 \\ \mathcal{O}\left((m^2)^s\right) + \mathcal{O}\left((m^2)^{r+s}\right), & \text{if } 0 \neq r \neq -s \neq 0 \end{cases} \quad (4.12)$$

That is, the double integral diverges worse than logarithmically if  $s < 0$ ,  $r \leq s = 0$  or  $r + s < 0$ . Of these only the case  $r = s = 0$ , which produces a double logarithm, appears in Eq. (4.11).

If  $\mathbf{k}_{1\perp}^2 > \mathbf{k}_{2\perp}^2$ , then instead

$$\frac{1}{t_2^2} = \frac{-(1-z_1)}{1-z_1+z_1z_2} \frac{1}{\mathbf{k}_{1\perp}^2} \sum_{n=0}^{\infty} \left( \frac{1-z_1}{(1-z_1+z_1z_2)(1-z_2)} \frac{\mathbf{k}_{2\perp}^2}{\mathbf{k}_{1\perp}^2} + \frac{2(1-z_1)}{1-z_1+z_1z_2} \frac{\mathbf{k}_{1\perp} \cdot \mathbf{k}_{2\perp}}{\mathbf{k}_{1\perp}^2} \right)^n \quad (4.13)$$

and the matrix element

$$\frac{1}{e^2} \left\langle |\mathcal{M}^{\gamma^* q \rightarrow q g g}|^2 \right\rangle_{\text{Ladder}}^{\mu\nu} = \frac{1}{\mathbf{k}_{1\perp}^4} \left[ A + B \left( \frac{\mathbf{k}_{2\perp}^2}{\mathbf{k}_{1\perp}^2} \right) + C \left( \frac{\mathbf{k}_{2\perp}^2}{\mathbf{k}_{1\perp}^2} \right)^2 + \dots \right] \quad (4.14)$$

contains at worst just logarithmically divergent terms. We thus find that the leading divergence comes from the region of phase space where the two transverse momenta are *strongly ordered*, with  $\mathbf{k}_{1\perp}^2 \ll \mathbf{k}_{2\perp}^2 \ll Q^2$ , producing the following leading logarithm contribution

$$\int d[\text{PS}]_3 \frac{1}{e^2} \left\langle |\mathcal{M}^{\gamma^* q \rightarrow q g g}|^2 \right\rangle_{\text{Ladder}}^{\mu\nu} \stackrel{\text{LL}}{=} \frac{\alpha_s^2}{2\pi} \frac{x}{Q^2} \int_x^1 \frac{dz_2}{z_2} C_F \left( \frac{1+z_2^2}{1-z_2} \right) \int_{x/z_2}^1 \frac{dz_1}{z_1} C_F \left( \frac{1+z_1^2}{1-z_1} \right) \delta\left(\xi - \frac{x}{z_1 z_2}\right) \times \frac{e_q^2}{2} \text{Tr}[\not{p}\gamma^\nu \not{p}\gamma^\mu] \frac{1}{2} \log^2\left(\frac{Q^2}{m^2}\right) \quad (4.15)$$

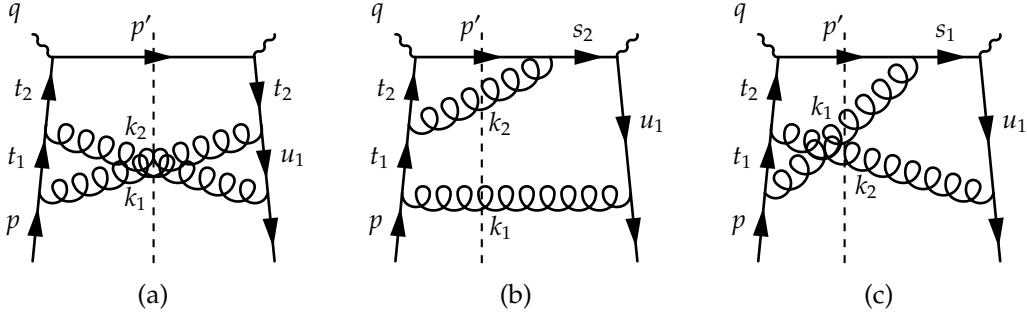


Figure 4.2: Non-ladder diagrams for two-gluon emission.

or, at the hadronic tensor level

$$\begin{aligned}
W_{\text{Q,2G-Ladder}}^{\mu\nu} &\stackrel{\text{LL}}{=} \frac{x}{4MQ^2} \text{Tr}[\not{P}\gamma^\nu(q+x\not{P})\gamma^\mu] \sum_q e_q^2 \frac{1}{2} \left(\frac{\alpha_s}{2\pi}\right)^2 \log^2\left(\frac{Q^2}{m^2}\right) \\
&\times \int_x^1 \frac{dz_2}{z_2} C_F \left(\frac{1+z_2^2}{1-z_2}\right) \int_{x/z_2}^1 \frac{dz_1}{z_1} C_F \left(\frac{1+z_1^2}{1-z_1}\right) f_q\left(\frac{x}{z_1 z_2}\right). \quad (4.16)
\end{aligned}$$

Here again we have taken the antiquark contributions from diagrams with reversed fermion lines to be included implicitly.

The soft divergences at limits  $z_1, z_2 \rightarrow 1$  get again regulated by self-energy insertions [1]. We omit, however, the discussion here. The general structure can still be seen from Eq. (4.16) and after substituting the terms in parentheses with appropriate plus distributions the contribution to the hadronic tensor reads

$$\frac{x}{4MQ^2} \text{Tr}[\not{P}\gamma^\nu(q+x\not{P})\gamma^\mu] \sum_q e_q^2 \frac{1}{2} \left(\frac{\alpha_s}{2\pi}\right)^2 \log^2\left(\frac{Q^2}{m^2}\right) P_{qq} \otimes P_{qq} \otimes f_q(x). \quad (4.17)$$

### 4.1.2 Non-ladder diagrams

Also at this order of  $\alpha_s$  various non-ladder diagrams, like those in Fig. 4.2 appear. But they all can easily be shown to be sub-leading. Consider the diagram in Fig. 4.2 (a), which contributes to the matrix element by

$$\begin{aligned}
\frac{1}{e^2} \left\langle |\mathcal{M}^{\nu q \rightarrow q g g}|^2 \right\rangle_{\text{Non-ladder,(a)}}^{\mu\nu} &= g_s^4 \frac{e_q^2}{2} \frac{1}{N_C} \text{Tr}[t^b t^a t^b t^a] \frac{1}{t_1^2 u_1^2 t_2^4} \\
&\times \sum_{\text{pol.}} \text{Tr}[\not{p} \not{\epsilon}_2 \not{t}_1 \not{\epsilon}_1 \not{t}_2 \gamma^\nu \not{p}' \gamma^\mu \not{t}_2 \not{\epsilon}_2^* \not{t}_1 \not{\epsilon}_1^*], \quad (4.18)
\end{aligned}$$

where  $t_1^2, t_2^2$  are as before and with  $u_1 = p - k_2$  we have

$$\frac{1}{u_1^2} = -\frac{(1-z_2)z_1}{\mathbf{k}_{2\perp}^2}. \quad (4.19)$$

When evaluating the trace in Eq. (4.18) we can use a similar trick as introduced in Sec. 3.1.3. First we notice that

$$t_1 \not{\epsilon}_1^* \not{p} = 2z_1 p \cdot \epsilon_1^* \not{p} + \mathcal{O}(k_{1\perp}) \quad (4.20)$$

and then use the polarization sum

$$\sum_{\text{pol.}} p \cdot \epsilon_1^* \not{\epsilon}_1 = \frac{2\beta_1}{1-z_1} \not{p} + \frac{1}{1-z_1} k_{1\perp} = \mathcal{O}(k_{1\perp}) \quad (4.21)$$

to see that no terms free from  $k_{1\perp}$  are contained in the trace. Likewise we have

$$\not{p} \not{\epsilon}_2^* \not{u}_1 = 2(1-z_1+z_1z_2)p \cdot \epsilon_2^* \not{p} + \mathcal{O}(k_{2\perp}), \quad \sum_{\text{pol.}} p \cdot \epsilon_2^* \not{\epsilon}_2 = \mathcal{O}(k_{2\perp}). \quad (4.22)$$

In the phase space region where  $\mathbf{k}_{1\perp}^2 < \mathbf{k}_{2\perp}^2$  the matrix element thus is of the form

$$\frac{1}{e^2} \left\langle \left| \mathcal{M}^{*q \rightarrow qgg} \right|^2 \right\rangle_{\text{Non-ladder,(a)}}^{\mu\nu} = \frac{1}{\mathbf{k}_{2\perp}^4} \left[ A + B \left( \frac{\mathbf{k}_{1\perp}^2}{\mathbf{k}_{2\perp}^2} \right) + C \left( \frac{\mathbf{k}_{1\perp}^2}{\mathbf{k}_{2\perp}^2} \right)^2 + \dots \right], \quad (4.23)$$

and when  $\mathbf{k}_{1\perp}^2 > \mathbf{k}_{2\perp}^2$

$$\frac{1}{e^2} \left\langle \left| \mathcal{M}^{*q \rightarrow qgg} \right|^2 \right\rangle_{\text{Non-ladder,(a)}}^{\mu\nu} = \frac{1}{\mathbf{k}_{1\perp}^4} \left[ A + B \left( \frac{\mathbf{k}_{2\perp}^2}{\mathbf{k}_{1\perp}^2} \right) + C \left( \frac{\mathbf{k}_{2\perp}^2}{\mathbf{k}_{1\perp}^2} \right)^2 + \dots \right], \quad (4.24)$$

neither of the series containing divergences higher than singly logarithmic order in integration over both transverse momenta. Similarly, any diagrams like those in Fig. 4.2 (b) and (c) can be shown to be subleading.

## 4.2 Additional ladder diagrams

The observation that leading logarithms appear only in ladder type diagrams holds also for processes other than the two-gluon emission [24]. We will now move on to calculate these contributions.

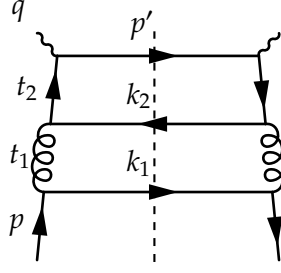


Figure 4.3: Two-rung ladder diagram with vertical gluons.

### 4.2.1 Vertical line gluons

Consider the process of initial quark and virtual photon going to a quark of the initial kind plus a quark–antiquark pair. The ladder diagram, shown in Fig. 4.3 has gluons in vertical lines and contributes to the matrix element with

$$\frac{1}{e^2} \left\langle |\mathcal{M}^{\gamma^* q' \rightarrow q' \bar{q} q}|^2 \right\rangle_{\text{Ladder}}^{\mu\nu} = g_s^4 \frac{e_q^2}{2} \frac{1}{N_C} \text{Tr}[t^a t^b] \text{Tr}[t^b t^a] \frac{1}{t_1^4 t_2^4} \text{Tr}[k_2 \gamma^\eta \not{t}_2 \gamma^\nu \not{p}' \gamma^\mu \not{t}_2 \gamma^\alpha] \times d_{\alpha\beta}(t_1) d_{\eta\omega}(t_1) \text{Tr}[\not{p} \gamma^\omega k_1 \gamma^\beta], \quad (4.25)$$

where the color factor simplifies to

$$\frac{1}{N_C} \text{Tr}[t^a t^b] \text{Tr}[t^b t^a] = T_F C_F. \quad (4.26)$$

A straightforward calculation shows that by using Eq. (B.8) the lower line in Eq. (4.25) can be written in a form

$$d_{\alpha\beta}(t_1) d_{\eta\omega}(t_1) \text{Tr}[\not{p} \gamma^\omega k_1 \gamma^\beta] = \frac{1 + (1 - z_1)^2}{z_1} \frac{2\mathbf{k}_{1\perp}^2}{z_1(1 - z_1)} \left( -g_{\alpha\eta} + \frac{p_\alpha n_\eta + p_\eta n_\alpha}{p \cdot n} \right) + \mathcal{O}(\mathbf{k}_{1\perp}^2 k_{1\perp}). \quad (4.27)$$

In contracting the leading part with the remaining trace we find

$$\not{t}_2 \gamma^\alpha k_2 \gamma^\eta \not{t}_2 \left( -g_{\alpha\eta} + \frac{p_\alpha n_\eta + p_\eta n_\alpha}{p \cdot n} \right) = 2 \frac{\mathbf{k}_{2\perp}^2}{1 - z_2} \left( (1 - z_2)^2 + z_2^2 \right) z_1 \not{p} + \dots, \quad (4.28)$$

where the ellipsis again contains all the different kinds of sub-leading terms.

Performing the phase space integration, the following leading logarithmic

term is produced

$$\begin{aligned} & \int d[\text{PS}]_3 \frac{1}{e^2} \left\langle |\mathcal{M}^{\gamma^* q' \rightarrow q' \bar{q} q}|^2 \right\rangle_{\text{Ladder}}^{\mu\nu} \\ & \stackrel{\text{LL}}{=} \frac{\alpha_s^2}{2\pi} \frac{x}{Q^2} \int_x^1 \frac{dz_2}{z_2} T_F \left( (1-z_2)^2 + z_2^2 \right) \int_{x/z_2}^1 \frac{dz_1}{z_1} C_F \left( \frac{1+(1-z_1)^2}{z_1} \right) \\ & \quad \times \delta \left( \xi - \frac{x}{z_1 z_2} \right) \frac{e_q^2}{2} \text{Tr}[\not{p} \gamma^\nu \not{t} \gamma^\mu] \frac{1}{2} \log^2 \left( \frac{Q^2}{m^2} \right). \end{aligned} \quad (4.29)$$

We find that this time no soft divergences appear, and thus this diagram contributes to the hadronic tensor by

$$\frac{x}{4MQ^2} \text{Tr}[\not{p} \gamma^\nu (\not{q} + x\not{p}) \gamma^\mu] \sum_{q,q'} e_q^2 \frac{1}{2} \left( \frac{\alpha_s}{2\pi} \right)^2 \log^2 \left( \frac{Q^2}{m^2} \right) P_{qg} \otimes P_{gq'} \otimes f_{q'}(x), \quad (4.30)$$

where we now found a new splitting function for gluon to quark transition

$$P_{gq}(z) \equiv C_F \left( \frac{1+(1-z)^2}{z} \right). \quad (4.31)$$

## 4.2.2 Gluon initiated diagrams

Let us next include the contribution from initial gluons. The ladder diagram in Fig. 4.4 (a) with the squared matrix element contribution

$$\frac{1}{e^2} \left\langle |\mathcal{M}^{\gamma^* g \rightarrow \bar{q} g q}|^2 \right\rangle_{\text{Ladder}}^{\mu\nu} = g_s^4 \frac{e_q^2}{2} \frac{1}{N_C^2 - 1} \text{Tr}[t^a t^b t^b t^a] \frac{1}{t_1^4 t_2^4} \text{Tr}[k_1 \not{\epsilon}_1^* t_1 \not{\epsilon}_2 t_2 \gamma^\nu \not{p}' \gamma^\mu t_2 \not{\epsilon}_2^* t_1 \not{\epsilon}_1], \quad (4.32)$$

where

$$\frac{1}{N_C^2 - 1} \text{Tr}[t^a t^b t^b t^a] = T_F C_F, \quad (4.33)$$

contains familiar elements. First, just as in Eq. (3.76), we notice that

$$\sum_{\text{pol.}} t_1 \not{\epsilon}_1^* k_1 \not{\epsilon}_1 t_1 = \frac{2}{1-z_1} \left( (1-z_1)^2 + z_1^2 \right) \mathbf{k}_{1\perp}^2 \not{p} + \mathcal{O}(\mathbf{k}_{1\perp}^2 k_{1\perp}), \quad (4.34)$$

and then exactly as in Eq. (4.6)

$$\sum_{\text{pol.}} t_2 \not{\epsilon}_2^* \not{p} \not{\epsilon}_2 t_2 = \frac{2}{1-z_2} \left( \frac{1+z_2^2}{1-z_2} \right) \mathbf{k}_{2\perp}^2 \not{p} + \dots \quad (4.35)$$

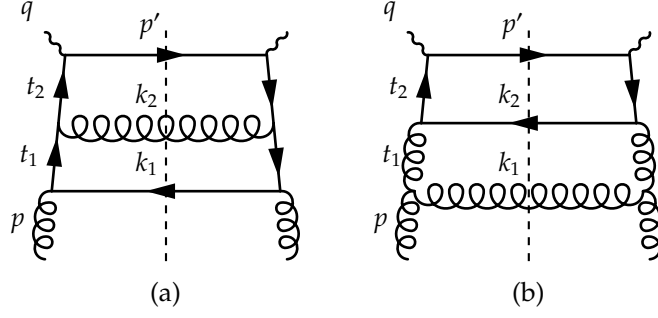


Figure 4.4: Two-rung ladder diagrams for initial gluon contribution.

After integrating over the phase space we have

$$\begin{aligned}
& \int d[\text{PS}]_3 \frac{1}{e^2} \left\langle |\mathcal{M}^{\gamma^* g \rightarrow \bar{q} g q}|^2 \right\rangle_{\text{Ladder}}^{\mu\nu} \\
& \stackrel{\text{LL}}{=} \frac{\alpha_s^2}{2\pi} \frac{x}{Q^2} \int_x^1 \frac{dz_2}{z_2} C_F \left( \frac{1+z_2^2}{1-z_2} \right) \int_{x/z_2}^1 \frac{dz_1}{z_1} T_F \left( (1-z_1)^2 + z_1^2 \right) \\
& \quad \times \delta \left( \xi - \frac{x}{z_1 z_2} \right) \frac{e_q^2}{2} \text{Tr}[\not{p} \gamma^\nu \not{t} \gamma^\mu] \frac{1}{2} \log^2 \left( \frac{Q^2}{m^2} \right). \quad (4.36)
\end{aligned}$$

Here again the soft divergence in the  $z_2$ -integration gets regulated by inclusion of a quark self-energy correction. Omitting the details, we just add the following term to the hadronic tensor

$$\frac{x}{4MQ^2} \text{Tr}[\not{P} \gamma^\nu (q + x\not{P}) \gamma^\mu] \sum_q e_q^2 \frac{1}{2} \left( \frac{\alpha_s}{2\pi} \right)^2 \log^2 \left( \frac{Q^2}{m^2} \right) P_{qq} \otimes P_{qg} \otimes f_g(x), \quad (4.37)$$

where the splitting functions are familiar from the previous order calculation.

The ladder diagram containing three-gluon vertices in Fig. 4.4 (b) gives

$$\begin{aligned}
\frac{1}{e^2} \left\langle |\mathcal{M}^{\gamma^* g \rightarrow \bar{q} \bar{q} q}|^2 \right\rangle_{\text{Ladder}}^{\mu\nu} &= g_s^4 \frac{e_q^2}{2} \frac{1}{N_C^2 - 1} \text{Tr}[t^a t^b] f^{acd} f^{bcd} \frac{1}{t_1^4 t_2^4} \sum_{\text{pol.}} \text{Tr}[k_2 \gamma^\eta t_2 \gamma^\nu \not{p}' \gamma^\mu t_2 \gamma^\alpha] \\
&\quad \times d_{\alpha\beta}(t_1) d_{\eta\omega}(t_1) \left\{ (k_1 + p)^\beta g^{\delta\gamma} + (t_1 - k_1)^\gamma g^{\beta\delta} - (t_1 + p)^\delta g^{\gamma\beta} \right\} \\
&\quad \times \left\{ (k_1 + p)^\omega g^{\sigma\rho} + (t_1 - k_1)^\rho g^{\omega\sigma} - (t_1 + p)^\sigma g^{\rho\omega} \right\} \varepsilon_{1\gamma}(p) \varepsilon_{1\rho}^*(p) \\
&\quad \times \varepsilon_{2\delta}^*(k_1) \varepsilon_{2\sigma}(k_1), \quad (4.38)
\end{aligned}$$

where the color factor can be simplified to

$$\frac{1}{N_C^2 - 1} \text{Tr}[t^a t^b] f^{acd} f^{bcd} = T_F C_A. \quad (4.39)$$

Here a somewhat lengthy calculation (which was here done with help of Mathematica) shows us that

$$\begin{aligned}
& d_{\alpha\beta}(t_1) d_{\eta\omega}(t_1) \left\{ \dots \right\}^{\beta\delta\gamma} \left\{ \dots \right\}^{\omega\sigma\rho} \sum_{\text{pol.}} \varepsilon_{1\gamma}(p) \varepsilon_{1\rho}^*(p) \varepsilon_{2\delta}^*(k_1) \varepsilon_{2\sigma}(k_1) \\
&= 2 \left( \frac{1-z_1}{z_1} + \frac{z_1}{1-z_1} + z_1(1-z_1) \right) \frac{2\mathbf{k}_{1\perp}^2}{z_1(1-z_1)} \left( -g_{\alpha\eta} + \frac{p_\alpha n_\eta + p_\eta n_\alpha}{p \cdot n} \right) + \mathcal{O}(\mathbf{k}_{1\perp}^2 k_{1\perp})
\end{aligned} \tag{4.40}$$

and the contraction with upper part of the diagram goes as in Eq. (4.28).

The phase space integration over Eq. (4.38) now yields

$$\begin{aligned}
& \int d[\text{PS}]_3 \frac{1}{e^2} \left\langle |\mathcal{M}^{g^*g \rightarrow g\bar{q}q}|^2 \right\rangle_{\text{Ladder}}^{\mu\nu} \\
& \stackrel{\text{LL}}{=} \frac{\alpha_s^2}{2\pi} \frac{x}{Q^2} \int_x^1 \frac{dz_2}{z_2} T_{\text{F}} \left( (1-z_2)^2 + z_2^2 \right) \int_{x/z_2}^1 \frac{dz_1}{z_1} 2C_{\text{A}} \left( \frac{1-z_1}{z_1} + \frac{z_1}{1-z_1} + z_1(1-z_1) \right) \\
& \quad \times \delta \left( \xi - \frac{x}{z_1 z_2} \right) \frac{e_q^2}{2} \text{Tr}[\not{p}\gamma^\nu \not{p}\gamma^\mu] \frac{1}{2} \log^2 \left( \frac{Q^2}{m^2} \right).
\end{aligned} \tag{4.41}$$

The appearance of a splitting function for gluon to gluon transition can be seen in the above expression, but we once again find a divergent  $1-z_1$  denominator which asks to be regulated. This will be done with a virtual correction coming from a gluon self-energy insertion, which we consider next.

### 4.2.3 Gluon self-energy

Just like we found for the quark, the gluon propagator obtains corrections from the field-strength renormalization factor

$$Z_g(p) D_{\mu\nu}(p) \stackrel{p^2 \rightarrow 0}{\sim} D_{\mu\nu}(p) + D_{\mu\eta}(p) [i\Pi^{\eta\omega}(p)] D_{\omega\nu}(p) + \dots, \tag{4.42}$$

where the gluon self-energy  $\Pi^{\eta\omega}$  we will now calculate at one-loop order.





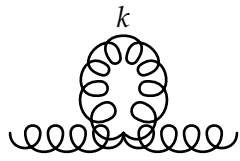
since we now have additional dependence on the gauge vector. Using the previously obtained methods and keeping only the terms leading to logarithmic divergences, a direct calculation (where again Mathematica was exploited) shows that

$$\begin{aligned}
A &= C_A \frac{\alpha_s}{2\pi} \int_0^1 d\alpha \left( \alpha^2 - \alpha + 2 - \frac{1}{\alpha} - \frac{1}{1-\alpha} \right) \log \left( \frac{\Lambda^2}{-\alpha(1-\alpha)p^2} \right) p^2 + \dots, \\
B &= C_A \frac{\alpha_s}{2\pi} \int_0^1 d\alpha \left( 2\alpha^2 - 2\alpha + \frac{1}{2} \right) \log \left( \frac{\Lambda^2}{-\alpha(1-\alpha)p^2} \right), \\
C &= C_A \frac{\alpha_s}{2\pi} \int_0^1 d\alpha \left( -3\alpha^2 + 3\alpha - \frac{5}{2} + \frac{1}{\alpha} + \frac{1}{1-\alpha} \right) \log \left( \frac{\Lambda^2}{-\alpha(1-\alpha)p^2} \right) \frac{p^2}{p \cdot n} + \dots, \\
D &= C_A \frac{\alpha_s}{2\pi} \int_0^1 d\alpha \left( 3\alpha^2 - 3\alpha + \frac{5}{2} - \frac{1}{\alpha} - \frac{1}{1-\alpha} \right) \log \left( \frac{\Lambda^2}{-\alpha(1-\alpha)p^2} \right) \frac{p^4}{(p \cdot n)^2} + \dots,
\end{aligned} \tag{4.54}$$

and thus we may write the gluon loop contribution to the self-energy in leading logarithm approximation as

$$\begin{aligned}
\Pi_g^{\eta\omega}(p) \stackrel{\text{LL}}{=} C_A \frac{\alpha_s}{2\pi} \log \left( \frac{\Lambda^2}{-p^2} \right) \left\{ \left( \frac{11}{6} - 2 \int_0^1 \frac{d\alpha}{1-\alpha} \right) (p^2 g^{\eta\omega} - p^\eta p^\omega) \right. \\
\left. + \left( 2 - 2 \int_0^1 \frac{d\alpha}{1-\alpha} \right) \left( p^\eta - \frac{p^2}{p \cdot n} n^\eta \right) \left( p^\omega - \frac{p^2}{p \cdot n} n^\omega \right) \right\}.
\end{aligned} \tag{4.55}$$

We should of course include the contribution from the tadpole diagram

$$\begin{aligned}
i \delta^{ba} \Pi_{g,\text{tadpole}}^{\eta\omega} &= a, \omega \text{  b, \eta \\
&= g_s^2 C_A \delta^{ba} \int \frac{d^4 k}{(2\pi)^4} \frac{1}{[k^2 + i\epsilon]} d_{\gamma\delta}(k) (2g^{\omega\eta} g^{\gamma\delta} - g^{\omega\delta} g^{\gamma\eta} - g^{\omega\gamma} g^{\eta\delta}) \\
&= \mathcal{O}(\Lambda^2),
\end{aligned} \tag{4.56}$$

but it contains no mass logarithms (the loop propagator is independent of the momentum  $p$ ) and thus does not contribute to our calculation.

## Full one-loop propagator

We have found the relevant part of gluon self-energy to be of the form

$$\Pi^{\eta\omega}(p) = \Pi_1 \left( p^2 g^{\eta\omega} - p^\eta p^\omega \right) + \Pi_2 \left( p^\eta - \frac{p^2}{p \cdot n} n^\eta \right) \left( p^\omega - \frac{p^2}{p \cdot n} n^\omega \right) \quad (4.57)$$

but when enclosing it between two propagators

$$D_{\mu\eta}(p) [i\Pi^{\eta\omega}(p)] D_{\omega\nu}(p) = \Pi_1 \frac{i}{p^2} \left( -g_{\mu\nu} + \frac{p_\mu n_\nu + p_\nu n_\mu}{p \cdot n} \right) - i\Pi_2 \frac{n_\mu n_\nu}{(p \cdot n)^2} \quad (4.58)$$

we can see that only  $\Pi_1$  contributes to the one-particle pole. The latter term would also lead to a loss of leading logarithm if the self-energy diagram is inserted in the middle of the ladder. The leading logarithmic part of the one loop correction to the gluon propagator hence is

$$\delta Z_g^{(1)}(p) \stackrel{\text{LL}}{=} \frac{\alpha_s}{2\pi} \log \left( \frac{\Lambda^2}{-p^2} \right) \left\{ C_A \left( \frac{11}{6} - 2 \int_0^1 \frac{d\alpha}{1-\alpha} \right) - \frac{2}{3} n_f T_F \right\}. \quad (4.59)$$

When inserted to the initial gluon leg of the one-rung ladder diagram in Fig. 3.5 (a), this produces a correction which regulates the soft divergence in Eq. (4.41). This procedure leads to the following contribution to the hadronic tensor

$$\frac{x}{4MQ^2} \text{Tr}[\not{p}\gamma^\nu(\not{q} + x\not{p})\gamma^\mu] \sum_q e_q^2 \frac{1}{2} \left( \frac{\alpha_s}{2\pi} \right)^2 \log^2 \left( \frac{Q^2}{m^2} \right) P_{qg} \otimes P_{gq} \otimes f_g(x), \quad (4.60)$$

where the splitting function for gluon to gluon transition is

$$P_{gg}(z) \equiv 2C_A \left( \frac{1-z}{z} + \frac{z}{(1-z)_+} + z(1-z) \right) + \left( \frac{11}{6} C_A - \frac{2}{3} n_f T_F \right) \delta(1-z). \quad (4.61)$$

## 4.3 Generalization to higher orders

A general structure begins to emerge. For every new order in  $\alpha_s$  the leading logarithms appear in the ladder diagrams with strongly ordered transverse momenta  $\mathbf{k}_{\perp 1}^2 \ll \dots \ll \mathbf{k}_{\perp n}^2 \ll Q^2$ . Combined with virtual corrections, their contribution to the cross section is free from soft divergences and every rung

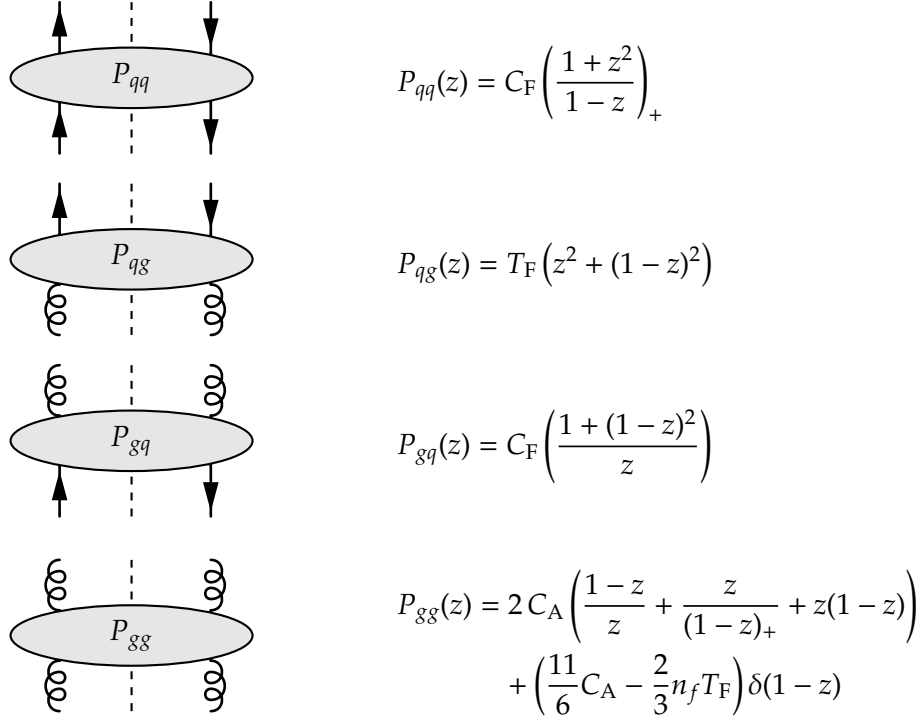


Figure 4.5: Splitting functions in LLA.

can be effectively replaced by convolution with a suitable splitting function (the four possibilities have been collected to Fig. 4.5) so that the  $\mathcal{O}(\alpha_s^n)$  contribution to the cross section becomes

$$\sum_{i,j,\dots,m,q} e_q^2 \frac{1}{n!} \left( \frac{\alpha_s}{2\pi} \right)^n \log^n \left( \frac{Q^2}{m^2} \right) \underbrace{P_{qm} \otimes \dots \otimes P_{ji}}_{n \text{ times}} \otimes f_i(x) \left( \frac{d\hat{\sigma}}{dQ^2 dx} \right)_{\text{Born}}, \quad (4.62)$$

where the factorial  $n!$  comes from the nested transverse momentum integrals. Summing over  $n$ , these contributions form an exponential series and the DIS cross section in leading logarithm approximation becomes

$$\frac{d\sigma}{dQ^2 dx} \stackrel{\text{LL}}{=} \sum_q e_q^2 (1 \ 0) \exp \left[ \frac{\alpha_s}{2\pi} \log \left( \frac{Q^2}{m^2} \right) \begin{pmatrix} P_{qq} & P_{qg} \\ P_{gq} & P_{gg} \end{pmatrix} \right] \otimes \begin{pmatrix} f_q \\ f_g \end{pmatrix} (x) \left( \frac{d\hat{\sigma}}{dQ^2 dx} \right)_{\text{Born}}, \quad (4.63)$$

where the  $(1,0)$  vector is present to ensure that the last splitting is into a quark.

### 4.3.1 Redefinition of parton distribution functions

We have seen that the collinear divergences appear when intermediate propagators get to on-shell (long lived) real particles. It would then make sense to include these long distance effects to the definition of the initial state. Let us define the *scale-dependent* parton distribution functions to all orders of collinear singularities and  $\alpha_s$  in the leading logarithm approximation the following way

$$\begin{pmatrix} f_q(x, Q^2) \\ f_g(x, Q^2) \end{pmatrix} \equiv \exp \left[ \frac{\alpha_s}{2\pi} \log \left( \frac{Q^2}{m^2} \right) \begin{pmatrix} P_{qq} & P_{qg} \\ P_{gq} & P_{gg} \end{pmatrix} \right] \otimes \begin{pmatrix} f_q \\ f_g \end{pmatrix}(x). \quad (4.64)$$

The DIS cross section then becomes

$$\frac{d\sigma}{dQ^2 dx} = \sum_q e_q^2 f_q(x, Q^2) \left( \frac{d\hat{\sigma}}{dQ^2 dx} \right)_{\text{Born}}. \quad (4.65)$$

This is a manifestation of the *factorization theorem* [27] which says that in hard processes the collinear divergences can be factored to scale dependent parton distribution functions and the remaining partonic cross section is free from divergences. This feature is not specific to leading order result obtained here, but applies also at higher orders.

The  $Q^2$  dependence of the quark density in Eq. (4.65) breaks the absolute Bjorken scaling that we found in the “naive” parton model. These *scaling violations* have been observed in DIS experiments (see [28]) and their explanation has been considered as one of the triumphs of QCD.

### 4.3.2 DGLAP evolution equations

Taking a  $Q^2$  derivative of the definition in Eq. (4.64) we find that the scale evolution of the parton densities are governed by the following *Dokshitzer–Gribov–Lipatov–Altarelli–Parisi* (DGLAP) *evolution equations* [3, 4, 5, 6]

$$Q^2 \frac{\partial}{\partial Q^2} \begin{pmatrix} f_q(x, Q^2) \\ f_g(x, Q^2) \end{pmatrix} = \frac{\alpha_s}{2\pi} \begin{pmatrix} P_{qq} & P_{qg} \\ P_{gq} & P_{gg} \end{pmatrix} \otimes \begin{pmatrix} f_q(Q^2) \\ f_g(Q^2) \end{pmatrix}(x). \quad (4.66)$$

Even though we derived the DGLAP evolution equations in the context of deeply inelastic scattering, the initial state evolution prior to a hard scattering should not depend on the nature of the hard interaction and hence the parton densities and their scale evolution should be *universal*, process independent.

Thus the same equations should apply to the scale evolution in hard processes in hadron–hadron collisions as well.

The form of Eq. (4.66) holds actually beyond leading logarithm approximation. Keeping track of the sub-leading contributions of the type  $\alpha_s^{n+1} \log^n(Q^2/m^2)$ ,  $\alpha_s^{n+2} \log^n(Q^2/m^2)$ , one can see that the splitting functions actually have higher order corrections

$$P_{ji} = P_{ji}^{(0)} + \frac{\alpha_s}{2\pi} P_{ji}^{(1)} + \left(\frac{\alpha_s}{2\pi}\right)^2 P_{ji}^{(2)} + \dots, \quad (4.67)$$

where the first term in the series are the leading logarithm splitting functions that we have derived here and the next-to-leading logarithm (NLL) terms have been derived in [29, 30] and NNLL in [31, 32]. While the leading logarithm quark to quark transition did not allow change in flavor,

$$P_{qq'}^{(0)} = 0 \quad \text{for } q' \neq q, \quad (4.68)$$

in higher orders this becomes possible and we should write the DGLAP equations in the form

$$Q^2 \frac{\partial}{\partial Q^2} \begin{pmatrix} f_q(x, Q^2) \\ f_g(x, Q^2) \end{pmatrix} = \frac{\alpha_s}{2\pi} \begin{pmatrix} P_{qq'} & P_{qg} \\ P_{gq'} & P_{gg} \end{pmatrix} \otimes \begin{pmatrix} f_{q'}(Q^2) \\ f_g(Q^2) \end{pmatrix}(x), \quad (4.69)$$

where  $f_q$  and the splitting functions are now understood to be vectors and matrices of appropriate dimensions.



# Chapter 5

## Concluding remarks

In this thesis we have gone through the derivation of DGLAP evolution equations in the context of deeply inelastic scattering using Sudakov decomposition in the light-cone gauge. In this formalism it was relatively easy to find the leading mass logarithms related to initial state collinear divergences and factor them into the definitions of parton distribution functions. We were able to find the full set of DGLAP equations with also the splitting functions  $P_{gq}$  and  $P_{gg}$  which are hard to achieve by other means. We also saw how the plus function prescription in  $P_{qq}$  and  $P_{gg}$  arise from the inclusion of virtual corrections without imposing momentum conservation requirements as was done originally in [5].

We find that after this resummation the same cross section formula as in the “naive” parton model holds in here with the “QCD-improved” parton model as long as the bare parton densities are replaced with  $Q^2$  dependent ones. One should notice that even though we have derived all the results in massless QCD where the  $\alpha_s \log(Q^2/m^2)$  terms approach infinity when the cut-off  $m^2$  is taken to zero, similar mass logarithms appear with massive quarks and become large for high values of  $Q^2$ , so their resummation is essential also in the massive theory.

We did not go through the full renormalization procedure of propagators and vertices in this thesis and thus also discussion about running of the coupling constant has been omitted. But one can show [1, 24] that the structure of the parton ladder is such that at the level of the DGLAP equations the renormalization just leads to a substitution  $\alpha_s \rightarrow \alpha_s(Q^2)$ . As we have seen the cut-off regularization causes some complications to the structure of ultraviolet divergences. To obtain a gauge invariant regularization one

could do the calculations in dimensional regularization while extracting the mass divergences by giving the initial partons a small virtuality  $p^2$ , a method effectively employed in [22].

It would have been instructive to show the cancellation of soft and final state collinear divergences explicitly rather than relying on to general principles (KLN theorem) at least in the first nontrivial order discussed in Chapter 3. But due to the extra divergences produced by the light-cone gauge one should be cautious when doing this. One can show in canonical quantization [33] that one should employ a so called *Mandelstam–Leibbrandt prescription* [34, 35] to the divergent  $k \cdot n$  denominators. We did not discuss this complication at all in our calculations since it should not have any effect to the initial state collinear divergences in the region of phase space where these denominators surely are nonvanishing. It is actually quite surprising how vaguely these “spurious” divergences are discussed in the literature. Most of the standard references where DGLAP equations are derived in light-cone gauge simply state that the dominant region of divergences is the one along the direction of the initial parton momentum with no reference at all to the possible complications caused by this gauge choice.

Now, with the evolution equations just derived, we can predict the parton densities at a scale  $Q^2$  if we know them at some lower scale  $Q_0^2$ . But it is of course not enough to have the evolution equations, for one needs to be able to solve them as well. A brief review on some of the used methods can be found in [36] and one very fast semianalytical approach [37] is also described in [1]. While we were able to derive the scale evolution from the theory of quantum chromodynamics, no prediction of the actual form of the parton densities can be given but these have to be determined experimentally. This is done through the methods of *global analysis*, details of which can be found in *e.g.* [1, 38]. For a given set of parton distribution functions, owing to their universality, we are now able to calculate numerical estimates for any hard cross section.

# Appendix A

## Quantum chromodynamics in the axial gauge

### A.1 QCD Lagrangian

Quantum chromodynamics (QCD) is a non-Abelian gauge theory with local  $SU(N_C)$  symmetry, where the number of colors is  $N_C = 3$ . The Lagrangian is given as

$$\mathcal{L} = \bar{\psi}(i\not{D} - m)\psi - \frac{1}{4}F_{\mu\nu}^a F^{a,\mu\nu}, \quad (\text{A.1})$$

where  $\psi$  is the quark multiplet,  $m$  the associated mass matrix and the covariant derivative is denoted as

$$D_\mu = \partial_\mu - ig_s A_\mu^a t^a, \quad (\text{A.2})$$

where  $A_\mu^a$  are the gluon fields and  $g_s$  denotes the strong coupling constant. The gluon field strength tensor is

$$F_{\mu\nu}^a = \partial_\mu A_\nu^a - \partial_\nu A_\mu^a + g_s f^{abc} A_\mu^b A_\nu^c. \quad (\text{A.3})$$

The matrices  $t^a$  are the  $SU(N_C)$  generators and  $f^{abc}$  the corresponding structure constants, properties of which are given in App. A.4.

The Lagrangian given in Eq. (A.1) is invariant under an infinitesimal local gauge transformation

$$\psi \rightarrow \psi + i\alpha^a t^a \psi, \quad A_\mu^a \rightarrow A_\mu^a + \frac{1}{g_s} \partial_\mu \alpha^a + f^{abc} A_\mu^b \alpha^c, \quad (\text{A.4})$$

consistently with the  $SU(N_C)$  symmetry. Quantization of such a theory requires removal of these unphysical degrees of freedom through gauge fixing [14]. In particular, it is not possible to define the gluon propagator without fixing the gauge [39]. For this reason, we add the following term

$$\mathcal{L}_{\text{gauge-fixing}} = -\frac{1}{2\lambda} (n^\mu A_\mu^a)^2 \quad (\text{A.5})$$

to the lagrangian in Eq. (A.1), thus reducing our theory to the class of axial gauges. The QCD Feynman rules [39, 40] for this gauge class are shown below.

## A.2 Feynman rules

### Propagators

$$i \xrightarrow[p]{} j = \delta_{ij} \frac{i}{\not{p} - m + i\epsilon} \quad (\text{A.6})$$

$$a, \alpha \text{ (wavy)} \xrightarrow[k]{} b, \beta = \delta^{ab} \frac{i}{k^2 + i\epsilon} \left\{ -g_{\alpha\beta} + \frac{k_\alpha n_\beta + k_\beta n_\alpha}{k \cdot n} - \frac{(n^2 + \lambda k^2) k_\alpha k_\beta}{(k \cdot n)^2} \right\} \quad (\text{A.7})$$

### Vertices

$$i \xrightarrow{a, \alpha} \text{ (wavy)} \text{ vertex } \xrightarrow{j} = -i g_s t_{ji}^a \gamma^\alpha \quad (\text{A.8})$$

$$c, \gamma \text{ (wavy)} \xrightarrow[k]{} \text{ (wavy)} \text{ vertex } \xrightarrow[b, \beta]{} = -g_s f^{abc} \left\{ (p - q)^\gamma g^{\alpha\beta} + (q - k)^\alpha g^{\beta\gamma} + (k - p)^\beta g^{\gamma\alpha} \right\} \quad (\text{A.9})$$

$$\begin{aligned} & \text{Diagram: } a, \alpha \text{ (wavy)} \text{ vertex } \xrightarrow{b, \beta} \text{ (wavy)} \text{ vertex } \xrightarrow{c, \gamma} \text{ (wavy)} \text{ vertex } \xrightarrow{d, \delta} \text{ (wavy)} \\ & = -i g_s^2 \left\{ f^{abe} f^{cde} (g^{\alpha\gamma} g^{\beta\delta} - g^{\alpha\delta} g^{\beta\gamma}) \right. \\ & \quad + f^{ace} f^{bde} (g^{\alpha\beta} g^{\gamma\delta} - g^{\alpha\delta} g^{\beta\gamma}) \\ & \quad \left. + f^{ade} f^{cbe} (g^{\alpha\gamma} g^{\beta\delta} - g^{\alpha\beta} g^{\delta\gamma}) \right\} \end{aligned} \quad (\text{A.10})$$

## Loop integrals

- For each loop with undetermined momentum  $k$ , integrate with  $\int \frac{d^4k}{(2\pi)^4}$ .
- For each closed fermion loop, multiply by  $-1$ .
- For each closed loop containing  $n$  identical bosons, multiply by  $\frac{1}{n!}$ .

## External lines

For an external quark with spin  $s$  and momentum  $p$

- in initial state, add a spinor  $u(p, s)$  on the right,
- in final state, add a spinor  $\bar{u}(p, s)$  on the left,

and for antiquark

- in initial state, add a spinor  $\bar{v}(p, s)$  on the left,
- in final state, add a spinor  $v(p, s)$  on the right.

For an external gluon with polarization  $\lambda$  and momentum  $k$

- in initial state, add a vector  $\varepsilon_\mu(k, \lambda)$ ,
- in final state, add a vector  $\varepsilon_\mu^*(k, \lambda)$ ,

where  $\mu$  is the Lorentz index of the vertex to which this line is connected.

## A.3 Spin and polarization sums

The spinors and polarization vectors from external lines obey the following sum rules

$$\begin{aligned} \sum_s u(p, s) \bar{u}(p, s) &= \not{p} + m, \\ \sum_s v(p, s) \bar{v}(p, s) &= \not{p} - m, \end{aligned} \tag{A.11}$$

$$\sum_{\lambda=1,2} \varepsilon_\mu(k, \lambda) \varepsilon_\nu^*(k, \lambda) = -g_{\mu\nu} + \frac{k_\mu n_\nu + k_\nu n_\mu}{k \cdot n} - n^2 \frac{k_\mu k_\nu}{(k \cdot n)^2}. \tag{A.12}$$

**Proof of Eq. (A.12):** We may produce the two physical polarization states  $\varepsilon_\mu(k, \lambda)$  ( $k^2 = 0, \lambda = 1, 2$ ) by introducing the Lorentz and gauge conditions

$$k \cdot \varepsilon(k, \lambda) = 0, \quad n \cdot \varepsilon(k, \lambda) = 0,$$

respectively. We can then parametrize the polarization sum with

$$\sum_{\lambda=1,2} \varepsilon_\mu(k, \lambda) \varepsilon_\nu^*(k, \lambda) = A g_{\mu\nu} + B n_\mu n_\nu + C(k_\mu n_\nu + k_\nu n_\mu) + D k_\mu k_\nu,$$

where contractions with  $k^\mu$  and  $n^\mu$  imply that

$$B = 0, \quad C = -\frac{A}{k \cdot n}, \quad D = n^2 \frac{A}{(k \cdot n)^2}.$$

Normalizing with  $\varepsilon(k, \lambda) \cdot \varepsilon(k, \lambda) = -1$  we find  $A = -1$  and thus

$$\sum_{\lambda=1,2} \varepsilon_\mu(k, \lambda) \varepsilon_\nu^*(k, \lambda) = -g_{\mu\nu} + \frac{k_\mu n_\nu + k_\nu n_\mu}{k \cdot n} - n^2 \frac{k_\mu k_\nu}{(k \cdot n)^2}.$$

## A.4 Color algebra

The  $SU(N_C)$  generator matrices  $t^a$  ( $a = 1, \dots, N_C^2 - 1$ ) satisfy the following commutation relation [39]:

$$[t^a, t^b] = i f^{abc} t^c \tag{A.13}$$

and are normalized with

$$\text{Tr}[t^a t^b] = T_F \delta^{ab}, \quad T_F = \frac{1}{2}. \tag{A.14}$$

We then have the following relations ( $i, j, k = 1, \dots, N_C$ ):

$$t_{ij}^a t_{jk}^a = C_F \delta_{ik}, \quad C_F = \frac{N_C^2 - 1}{2N_C}, \tag{A.15}$$

$$f^{abc} f^{abd} = C_A \delta^{cd}, \quad C_A = N_C, \tag{A.16}$$

where in the case of  $N_C = 3$  the weights of the Casimir operator in the fundamental and adjoint representations are,

$$C_F = \frac{4}{3}, \quad C_A = 3, \tag{A.17}$$

respectively.

# Appendix B

## Kinematics

### B.1 Sudakov decomposition

When extracting collinear divergences, it is convenient to parametrize momenta using the Sudakov decomposition [16]. For a generic four-momentum  $k$  we may write

$$k = \alpha p + \beta n + k_{\perp}, \quad (\text{B.1})$$

where  $p$  and  $n$  are arbitrary four-momenta (but have to satisfy  $p \cdot n \neq 0$ ), and  $k_{\perp}$  is chosen such that

$$p \cdot k_{\perp} = n \cdot k_{\perp} = 0. \quad (\text{B.2})$$

If  $n^2 = 0$ , as is often convenient to choose, then by squaring Eq. (B.1) we find (for non-zero  $\alpha$ )

$$\beta = \frac{k^2 - k_{\perp}^2 - \alpha^2 p^2}{2\alpha p \cdot n}. \quad (\text{B.3})$$

Thus, the vector  $k$  becomes parametrized by its virtuality  $k^2$ , its transverse component  $k_{\perp}$ , and  $\alpha$ , the fraction of momentum along  $p$ .

In a frame chosen so that

$$p = (p^0, 0, 0, p^3), \quad n = (n^0, 0, 0, n^3) \quad (\text{B.4})$$

we have

$$k = (\alpha p^0 + \beta n^0, \mathbf{k}_{\perp}, \alpha p^3 + \beta n^3), \quad \mathbf{k}_{\perp}^2 = -k_{\perp}^2 \quad (\text{B.5})$$

and the  $k$ -differential can be written as

$$\begin{aligned}
d^4k &= d\alpha dk^2 d^2\mathbf{k}_\perp \left| \begin{array}{cc} p^0 + \frac{d\beta}{d\alpha}n^0 & p^3 + \frac{d\beta}{d\alpha}n^3 \\ \frac{d\beta}{dk^2}n^0 & \frac{d\beta}{dk^2}n^3 \end{array} \right| \\
&= d\alpha dk^2 d^2\mathbf{k}_\perp \left| \frac{d\beta}{dk^2} \right| |p^0n^3 - p^3n^0| \\
&= d\alpha dk^2 d^2\mathbf{k}_\perp \left| \frac{1}{2\alpha p \cdot n} \right| |p \cdot n| \\
&= \frac{d\alpha}{2|\alpha|} dk^2 d^2\mathbf{k}_\perp,
\end{aligned} \tag{B.6}$$

where we used the property that since  $n$  is a null vector, we have  $n^3 = \pm n^0$  in this frame.

## B.2 Transverse momentum tensor integrals

When integrating over the transverse momentum plane we obtain following identities

$$\int d^2\mathbf{k}_\perp \frac{k_\perp^\mu}{\mathcal{D}(\mathbf{k}_\perp^2)} = 0, \tag{B.7}$$

$$\int d^2\mathbf{k}_\perp \frac{k_\perp^\mu k_\perp^\eta}{\mathcal{D}(\mathbf{k}_\perp^2)} = \frac{1}{2} \left( -g^{\mu\eta} + \frac{p^\mu n^\eta + p^\eta n^\mu}{p \cdot n} - p^2 \frac{n^\mu n^\eta}{(p \cdot n)^2} \right) \int d^2\mathbf{k}_\perp \frac{\mathbf{k}_\perp^2}{\mathcal{D}(\mathbf{k}_\perp^2)}, \tag{B.8}$$

where the denominator function  $\mathcal{D}$  only depends on the square of the transverse momentum and not on the individual components separately.

**Proof of Eq. (B.7):** In the following vector integral

$$I_{\mathbf{k}_\perp}^\mu \equiv \int d^2\mathbf{k}_\perp \frac{k_\perp^\mu}{\mathcal{D}(\mathbf{k}_\perp^2)},$$

the only non-scalar objects the result can depend on are the vectors  $p$  and  $n$  parametrizing the left-over momentum space. Thus, by the Lorentz symmetry, the vector integral can be decomposed as

$$I_{\mathbf{k}_\perp}^\mu = Ap^\mu + Bn^\mu.$$

Contracting with  $p^\mu, n^\mu$  and requiring  $n^2 = 0$  we find

$$A = \frac{1}{p \cdot n} n_\mu I_{\mathbf{k}_\perp}^\mu = 0,$$

$$B = \frac{1}{p \cdot n} p_\mu I_{\mathbf{k}_\perp}^\mu - \frac{p^2}{p \cdot n} A = 0.$$

Hence

$$I_{\mathbf{k}_\perp}^\mu = 0.$$

**Proof of Eq. (B.8):** Following the same reasoning as above, the rank-2 tensor integral

$$I_{\mathbf{k}_\perp}^{\mu\eta} \equiv \int d^2\mathbf{k}_\perp \frac{k_\perp^\mu k_\perp^\eta}{\mathcal{D}(\mathbf{k}_\perp^2)}$$

can be decomposed as

$$I_{\mathbf{k}_\perp}^{\mu\eta} = A g^{\mu\eta} + B p^\mu p^\eta + C(p^\mu n^\eta + p^\eta n^\mu) + D n^\mu n^\eta.$$

Assuming  $n^2 = 0$ , the contraction with  $p^\mu, n^\mu$  yields a set of equations, which can be solved for

$$B = 0, \quad C = -\frac{A}{p \cdot n}, \quad D = p^2 \frac{A}{(p \cdot n)^2}.$$

Then, finally, from the contraction with  $g^{\mu\eta}$ , we find

$$A = -\frac{1}{2} \int d^2\mathbf{k}_\perp \frac{\mathbf{k}_\perp^2}{\mathcal{D}(\mathbf{k}_\perp^2)},$$

and thus

$$I_{\mathbf{k}_\perp}^{\mu\eta} = \frac{1}{2} \left( -g^{\mu\eta} + \frac{p^\mu n^\eta + p^\eta n^\mu}{p \cdot n} - p^2 \frac{n^\mu n^\eta}{(p \cdot n)^2} \right) \int d^2\mathbf{k}_\perp \frac{\mathbf{k}_\perp^2}{\mathcal{D}(\mathbf{k}_\perp^2)}.$$



# Bibliography

- [1] Hannu Paukkunen, “Global analysis of nuclear parton distribution functions at leading and next-to-leading order perturbative QCD”, PhD thesis, University of Jyväskylä, 2009.
- [2] H. David Politzer, “Asymptotic Freedom: An Approach to Strong Interactions”, *Phys. Rept.* 14 (1974) 129.
- [3] L. N. Lipatov, “The parton model and perturbation theory”, *Sov. J. Nucl. Phys.* 20 (1975), [*Yad. Fiz.* 20 (1974) 181] 94.
- [4] V. N. Gribov and L. N. Lipatov, “Deep inelastic e p scattering in perturbation theory”, *Sov. J. Nucl. Phys.* 15 (1972), [*Yad. Fiz.* 15 (1972) 781] 438.
- [5] Guido Altarelli and G. Parisi, “Asymptotic Freedom in Parton Language”, *Nucl. Phys.* B126 (1977) 298.
- [6] Yuri L. Dokshitzer, “Calculation of the Structure Functions for Deep Inelastic Scattering and e+ e- Annihilation by Perturbation Theory in Quantum Chromodynamics.”, *Sov. Phys. JETP* 46 (1977), [*Zh. Eksp. Teor. Fiz.* 73 (1977) 1216] 641.
- [7] K. J. Eskola, “Perturbative QCD, PDFs and hard processes”, Lecture notes, University of Jyväskylä, 2014.
- [8] Michael E. Peskin and Daniel V. Schroeder, *An Introduction to quantum field theory*, Perseus Books, 1995.
- [9] George F. Sterman, *An Introduction to quantum field theory*, Cambridge University Press, 1993.
- [10] Richard P. Feynman, “Very high-energy collisions of hadrons”, *Phys. Rev. Lett.* 23 (1969) 1415.
- [11] J. D. Bjorken and Emmanuel A. Paschos, “Inelastic Electron Proton and  $\gamma$ -Proton Scattering, and the Structure of the Nucleon”, *Phys. Rev.* 185 (1969) 1975.
- [12] R. E. Cutkosky, “Singularities and discontinuities of Feynman amplitudes”, *J. Math. Phys.* 1 (1960) 429.

- [13] L. D. Faddeev and V. N. Popov, "Feynman Diagrams for the Yang-Mills Field", *Phys. Lett.* B25 (1967) 29.
- [14] George Leibbrandt, "Introduction to Noncovariant Gauges", *Rev. Mod. Phys.* 59 (1987) 1067.
- [15] S. Mandelstam, "Determination of the pion - nucleon scattering amplitude from dispersion relations and unitarity. General theory", *Phys. Rev.* 112 (1958) 1344.
- [16] V. V. Sudakov, "Vertex parts at very high-energies in quantum electrodynamics", *Sov. Phys. JETP* 3 (1956) 65.
- [17] Yuri L. Dokshitzer, Dmitri Diakonov, and S. I. Troian, "Hard Processes in Quantum Chromodynamics", *Phys. Rept.* 58 (1980) 269.
- [18] T. Kinoshita, "Mass singularities of Feynman amplitudes", *J. Math. Phys.* 3 (1962) 650.
- [19] T. D. Lee and M. Nauenberg, "Degenerate Systems and Mass Singularities", *Phys. Rev.* 133 (1964) B1549.
- [20] D. Amati, R. Petronzio, and G. Veneziano, "Relating Hard QCD Processes Through Universality of Mass Singularities", *Nucl. Phys.* B140 (1978) 54.
- [21] H. Lehmann, K. Symanzik, and W. Zimmermann, "On the formulation of quantized field theories", *Nuovo Cim.* 1 (1955) 205.
- [22] D. J. Pritchard and W. James Stirling, "QCD Calculations in the Light Cone Gauge. 1", *Nucl. Phys.* B165 (1980) 237.
- [23] Guido Altarelli, R. Keith Ellis, and G. Martinelli, "Large Perturbative Corrections to the Drell-Yan Process in QCD", *Nucl. Phys.* B157 (1979) 461.
- [24] Yuri L. Dokshitzer et al., *Basics of perturbative QCD*, Editions Frontieres, 1991.
- [25] T. Muta, *Foundations of quantum chromodynamics: An Introduction to perturbative methods in gauge theories*, World Scientific, 1987.
- [26] Gerard 't Hooft and M. J. G. Veltman, "Regularization and Renormalization of Gauge Fields", *Nucl. Phys.* B44 (1972) 189.
- [27] John C. Collins, Davison E. Soper, and George F. Sterman, "Factorization of Hard Processes in QCD", *Adv. Ser. Direct. High Energy Phys.* 5 (1989) 1.
- [28] K. A. Olive et al., "Review of Particle Physics", *Chin. Phys.* C38 (2014) 090001.
- [29] W. Furmanski and R. Petronzio, "Singlet Parton Densities Beyond Leading Order", *Phys. Lett.* B97 (1980) 437.
- [30] G. Curci, W. Furmanski, and R. Petronzio, "Evolution of Parton Densities Beyond Leading Order: The Nonsinglet Case", *Nucl. Phys.* B175 (1980) 27.

- [31] A. Vogt, S. Moch, and J. A. M. Vermaseren, "The Three-loop splitting functions in QCD: The Singlet case", *Nucl. Phys.* B691 (2004) 129.
- [32] S. Moch, J. A. M. Vermaseren, and A. Vogt, "The Three loop splitting functions in QCD: The Nonsinglet case", *Nucl. Phys.* B688 (2004) 101.
- [33] A. Bassetto et al., "Yang-Mills Theories in the Light Cone Gauge", *Phys. Rev.* D31 (1985) 2012.
- [34] Stanley Mandelstam, "Light Cone Superspace and the Ultraviolet Finiteness of the N=4 Model", *Nucl. Phys.* B213 (1983) 149.
- [35] George Leibbrandt, "The Light Cone Gauge in Yang-Mills Theory", *Phys. Rev.* D29 (1984) 1699.
- [36] Jiri Chyla, "Quarks, partons and Quantum Chromodynamics", Lecture notes, Prague, Inst. Phys., 2009.
- [37] Pietro Santorelli and Egidio Scrimieri, "A Semianalytical method to evolve parton distributions", *Phys. Lett.* B459 (1999) 599.
- [38] A. D. Martin et al., "Parton distributions for the LHC", *Eur. Phys. J.* C63 (2009) 189.
- [39] R. Keith Ellis, W. James Stirling, and B. R. Webber, *QCD and collider physics*, Cambridge University Press, 1996.
- [40] R. D. Field, *Applications of Perturbative QCD*, Addison-Wesley, 1989.